

Thermal width and quarkonium dissociation by inelastic parton scattering

Nora Brambilla^a Miguel Ángel Escobedo^a Jacopo Ghiglieri^b Antonio Vairo^a

^a*Physik-Department, Technische Universität München,
James-Frank-Str. 1, 85748 Garching, Germany*

^b*Department of Physics, McGill University, 3600 rue University, Montréal QC H3A 2T8, Canada*

E-mail: nora.brambilla@ph.tum.de, miguel.escobedo@ph.tum.de,
jacopo.ghiglieri@physics.mcgill.ca, antonio.vairo@ph.tum.de

ABSTRACT: In a weak-coupling effective field theory framework we study quarkonium dissociation induced by inelastic scattering with partons in the medium. This is the dominant dissociation process for temperatures such that the Debye mass is larger than the binding energy. We evaluate the dissociation cross section and the corresponding thermal decay width. At leading order we derive a convolution formula relating the two, which is consistent with the optical theorem and QCD at finite temperature. Bound state effects are systematically included. They add contributions to the cross section and width that are beyond a quasi-free approximation, whose validity is critically reviewed. For temperatures such that the Debye mass is smaller than the binding energy, the dominant dissociation mechanism is gluo-dissociation consisting in quarkonium dissociation induced by the absorption of a gluon from the medium. We calculate the gluo-dissociation cross section and width at next-to-leading-order accuracy.

KEYWORDS: Quarkonium, Heavy Ion Phenomenology

Contents

1	Introduction	1
2	General considerations on dissociation by inelastic parton scattering	3
3	General considerations on the EFT approach	7
4	The $T \gg mv \sim m_D$ case	8
4.1	The $mv \gg m_D$ case	11
4.2	Comparison with the literature	14
5	The $T \sim mv \gg m_D$ case	16
6	The $mv \gg T \gg m_D \gg E$ case	19
6.1	Comparison with the literature	22
7	The $mv \gg T \gg E \gg m_D$ case	23
7.1	Gluo-dissociation	25
7.2	Dissociation by inelastic parton scattering	26
7.3	Comparison with the literature	28
8	Conclusions	28

1 Introduction

Heavy-quarkonium suppression, first proposed in [1] as a signal of deconfinement, has been observed at SPS, RHIC and recently at LHC [2–5]. Although the current understanding is that the observed quarkonium suppression cannot be explained by cold nuclear matter effects alone [3], the hot nuclear matter mechanism responsible for it is still under investigation. In [1], it was suggested that heavy quark-antiquark ($Q\bar{Q}$) bound states dissociate in a hot thermal bath because of colour screening of the $Q\bar{Q}$ potential induced by the medium. In [6], another dissociation mechanism was identified in the Landau-damping phenomenon. Implications of the Landau-damping mechanism on the quarkonium dynamics, and anisotropic generalizations thereof, can be found in [7–10].

In the context of real-time thermal field theory, quarkonium in a thermal bath may be studied by taking advantage of the non-relativistic and thermal energy scales that characterize the system. The scales typical of a non-relativistic bound state are the heavy-quark mass m , the momentum transfer or inverse radius $1/r \sim mv$ and the binding energy $E \sim mv^2$. Because $v \ll 1$ is the relative velocity of the heavy quarks, these scales are

hierarchically ordered: $m \gg mv \gg mv^2$. The thermal bath is characterized by a temperature T and a Debye screening mass m_D . In a weakly-coupled plasma, $m_D \sim gT$ and also the thermal scales are ordered: $T \gg m_D$. Integrating out systematically degrees of freedom associated with the highest energy scale leads to a hierarchy of low-energy effective field theories (EFTs) [11, 12]. The ultimate of these EFTs can be interpreted as a finite-temperature version of potential non-relativistic QCD (pNRQCD) [13, 14]. Potential non-relativistic QCD describes the quarkonium dynamics through potentials and low-energy interactions. Thermal corrections affect both the real and the imaginary parts of the potentials. Thermal corrections to the real part of the colour-singlet potential may lead to the colour-screening phenomenon described by Matsui and Satz, whereas thermal corrections to the imaginary part of the colour-singlet potential induce a thermal width. Several mechanisms may contribute to the imaginary part of the potential. One of these is precisely the Landau-damping mechanism identified in [6]. In [11, 15], it was shown that the thermal width induced by the Landau-damping phenomenon is the principal source of quarkonium dissociation at weak coupling, responsible for keeping the quarkonium dissociated even at temperatures where colour screening on the real part of the potential has faded away. Moreover, lattice studies have shown that the potential may have a sizeable imaginary part also at strong coupling [16–18].

In a non-EFT framework, quarkonium decay widths induced by scattering with the medium constituents have been studied since long time (see for instance [19–22] and references therein). At leading order, two different dissociation mechanisms were identified: *gluo-dissociation* [23, 24] and *dissociation by inelastic parton scattering* [25, 26]. In the former case, the bound state absorbs a sufficiently energetic gluon of the medium and dissociates into an unbound colour-octet $Q\bar{Q}$ pair. The gluon is physical, in the sense that its momentum is either light-like or time-like if it acquires an effective mass propagating through the medium. In the latter case a light parton of the medium, gluon or quark, scatters off the bound state by exchanging gluons, resulting again in its dissociation into an unbound colour octet. The momentum of the exchanged gluon is in this case space-like. In both cases, the decay widths were obtained by convoluting the $T = 0$ cross section for the scattering process, possibly with some ad-hoc finite-temperature modifications, with the thermal distribution of the incoming parton.

In the EFT framework, thermal decay widths have been investigated over a wide range of temperatures [11, 12, 27]. In [12], two mechanisms contributing at leading order to the quarkonium decay width were identified: *singlet-to-octet thermal breakup* and *Landau damping*. In the power-counting of the EFT, it was shown that the latter dominates over the former as long as $m_D \gg E$. These two mechanisms are not independent from those identified earlier without EFT methods. In terms of elementary processes, the singlet-to-octet thermal breakup corresponds to gluon-dissociation and the Landau-damping mechanism to dissociation by inelastic parton scattering [28]. Beyond leading order the two mechanisms are intertwined and distinguishing between them becomes unphysical, whereas the physical quantity is the total width.

The equivalence of the singlet-to-octet thermal breakup process to gluo-dissociation has been analyzed at leading order in [29]. There the singlet-to-octet thermal breakup

width and the gluo-dissociation cross section have been computed for several temperature regimes. The decay width in the regime $mv \gg T \gg E \gg m_D$, which has been suggested to be of relevance for $\Upsilon(1S)$ suppression at the LHC [30], agrees with the one previously calculated in [27]. Moreover it is consistent with the lattice QCD findings of [31]. The gluo-dissociation cross section agrees in the large- N_c limit with the cross section derived in [32], which is often used in the literature. The gluo-dissociation cross section has been confirmed by [33].

In this paper, we will perform a similar analysis for what concerns the relation between the Landau-damping mechanism and the dissociation by inelastic parton scattering. We will compute in an EFT framework the dissociation cross section and the corresponding thermal width in different temperature regimes and relate the results with the existing literature. The cross section for dissociation by inelastic parton scattering was computed in [34] neglecting bound-state effects, and more recently (but in a different validity region) in [35]. The relevance of this process for heavy-ion collisions was realized in [25] and since then phenomenological expressions for the quarkonium decay width due to dissociation by inelastic parton scattering in the medium have been widely used in the literature (see [26, 36–40]). As this process gives the dominant contribution to the decay width for $m_D \gg E$, which is the temperature regime at which quarkonium dissociates, validating those expressions from QCD is of utmost phenomenological relevance. In fact, we will show that the convolution formula commonly used in the literature to connect the dissociation cross section to the decay width does not follow from the optical theorem applied to QCD at finite temperature and we will suggest a different one. Furthermore, we will argue that neglecting bound-state effects is not a valid approximation in a weak-coupling setting below the quarkonium dissociation temperature.

The paper is organized as follows. In section 2, we give some general arguments based on the optical theorem in thermal field theory and on effective field theories to derive a formula relating the dissociation cross section to the decay width. In section 3, we illustrate the basics of pNRQCD. In section 4, we study the cross section and width in the temperature regime $T \gg mv \sim m_D$ and in section 5 we consider the regime $T \sim mv \gg m_D$. In section 6, we focus on the temperature regime $mv \gg T \gg m_D \gg E$, where a multipole expansion in the temperature is possible. We obtain a colour dipole cross section and we study the validity region of this approximation. In section 7, we analyze the temperature regime $mv \gg T \gg E \gg m_D$, where, as we shall show, both gluo-dissociation and dissociation by parton scattering get a contribution from the same EFT diagram. Hence, we compute next-to-leading-order (NLO) corrections to the gluo-dissociation cross section. Finally, in section 8 we draw some conclusions.

2 General considerations on dissociation by inelastic parton scattering

It has been suggested in [25] and used in most of the following literature on the subject that the width Γ_{HQ} for dissociation by inelastic parton scattering of a heavy quarkonium,

HQ, at rest with respect to the thermal bath could be expressed by the convolution formula

$$\Gamma_{\text{HQ}} = \sum_p \int_{q_{\min}} \frac{d^3 q}{(2\pi)^3} f_p(q) \sigma_p^{\text{HQ}}(q), \quad (2.1)$$

where the sum runs over the different species of incoming light partons, p , with momentum $q = |\mathbf{q}|$, and the distribution functions, f_p , are the Bose–Einstein distribution $n_B(q) = 1/(\exp(q^0/T) - 1)$ for gluons and the Fermi–Dirac distribution $n_F(q) = 1/(\exp(q^0/T) + 1)$ for light quarks. The momentum q_{\min} is the minimum incoming momentum necessary to dissociate the bound state. The distribution functions are convoluted with σ_p^{HQ} , a quantity identified with the parton-heavy-quarkonium dissociation cross section in the medium. In [25] and related literature, σ_p^{HQ} has been approximated by $2\sigma_p^Q$, where σ_p^Q is the cross section of the zero-temperature process $pQ \rightarrow pQ$. Because this approximation neglects bound-state effects, it is called quasi-free.¹ The scattering process $pQ \rightarrow pQ$ receives at leading order in perturbation theory contributions from the four diagrams shown in figure 1; these were computed in [34]. It is the cross section computed in [34] that is commonly used in eq. (2.1). Besides the distribution functions, additional thermal effects are usually added to (2.1) in the form of momentum-independent thermal masses affecting the dispersion relations and propagators of the light partons. Thermal masses also provide a cut off for the infrared divergences typically affecting the forward scattering amplitude.

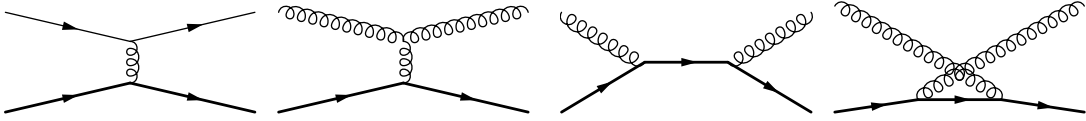


Figure 1. Tree level diagrams contributing to $pQ \rightarrow pQ$, where p is a parton and Q a heavy quark. Thick lines stand for heavy quarks, curly lines for gluons and thin lines for light quarks.

Our purpose is to scrutinize eq. (2.1) and the quasi-free approximation in the light of QCD at finite temperature. We start by making some general considerations about the form of the dissociation formula. A quantitative treatment in a weak-coupling regime will be developed in the next sections. The dissociation process we are considering happens when partons in the thermal bath, i.e. partons with momentum and energy of the order of the temperature, scatter off the quarkonium and dissociate it by exchanging space-like gluons. First, we observe that by performing the calculation in Coulomb gauge, we only need to take into account transverse gluons, A_i , as external gauge fields. The reason is that in Coulomb gauge temporal gluons, A_0 , do not thermalize at the scale T ; moreover their spectral density vanishes and hence they do not contribute to cut diagrams. The Coulomb gauge is therefore a convenient gauge for the calculation, and we will adopt it for the rest of the paper. Next, we assume that the heavy-quark mass is much larger than the temperature: $m \gg T$. This implies that one can integrate out hard modes with

¹ In the literature, dissociation by inelastic parton scattering is sometimes called for conciseness quasi-free dissociation, after the approximation used for its computation.

energy and momentum of order m from QCD neglecting thermal effects, and replace QCD by non-relativistic QCD (NRQCD) [41, 42] as the fundamental theory. In NRQCD, the leading interaction between heavy quarks and gluon fields A_i is encoded in dimension-five operators; each of these interactions brings a suppression factor proportional to T/m . We conclude that in Coulomb gauge the last two diagrams in figure 1 are at least suppressed by a factor T/m with respect to the first two and can be neglected at leading order.

Whenever the momentum carried by the gluon coupled to the heavy quark is larger than or of the same order as mv , based on the same argument given in the previous paragraph we can argue that the leading-order contribution of the first two diagrams in figure 1 comes from the coupling of a temporal gluon to the heavy quark. This case will be relevant for section 4 and 5. Whenever the momentum carried by the gluon coupled to the heavy quark is smaller than mv , but larger than the binding energy, the contribution of the temporal gluons cancels at leading-order in the multipole expansion in the square of the amplitude of the first two diagrams of figure 1 and the corresponding antiquark diagrams. This was noted in [12] and will be shown again in the following. Nevertheless, also in this case we may neglect at leading order the coupling of a transverse gluon to the heavy quark. The reason is that its contribution is proportional to the binding energy of the quarkonium, and this is subleading with respect to the momentum carried by the gluon. This case will be relevant for most of the temperature regions studied in the paper. Finally, whenever the momentum carried by the gluon coupled to the heavy quark is of the same order as the binding energy, the contribution coming from a transverse gluon coupled to the heavy quark will be at next-to-leading order in the multipole expansion as important as the one coming from a temporal gluon and we will need to consider them both. This case will be relevant only for section 7.

Since in all cases only the first two diagrams in figure 1 contribute at non-vanishing leading order, it follows from the optical theorem that the dissociation cross section is proportional to the imaginary part of $iD^{\mu\nu}$, where $D^{\mu\nu}$ is the gluon propagator. The gluon propagator may be computed in the so-called real-time formalism of thermal field theory (see e.g. [43]). A feature of this formalism is that the degrees of freedom double: while external particles are only of type “1”, i.e. they live on the time-ordered branch of the Schwinger–Keldysh contour, in loops one has to consider also particles of type “2”, i.e. particles located on the anti-time-ordered branch. It has been shown in [12, 44] that under the condition $m \gg T$ heavy quarks do not thermalize up to exponentially suppressed contributions and can be treated as external probes. Hence, all vertices involving heavy quarks are of type “1” and, as a consequence, one needs to consider only the imaginary part of the “11” component of the gluon propagator coupled to the heavy quark. In general, this can be written in terms of an advanced (A), retarded (R) and symmetric (S) propagator as

$$D_{11}^{\mu\nu}(k_0, k) = \frac{1}{2} [D_R^{\mu\nu}(k_0, k) + D_A^{\mu\nu}(k_0, k) + D_S^{\mu\nu}(k_0, k)] , \quad (2.2)$$

where throughout the paper italic letters refer to the modulus of the spatial momentum, i.e. $k = |\mathbf{k}|$. Since $(iD_R^{\mu\nu})^* = iD_A^{\mu\nu}$, the discontinuity $iD_{11}^{\mu\nu} - (iD_{11}^{\mu\nu})^*$ is equal to $iD_S^{\mu\nu}$, which is in turn related to the retarded and advanced propagators through $D_S^{\mu\nu}(k_0, k) = [1 +$

$2n_B(|k_0|)] \operatorname{sgn}(k_0) [D_R^{\mu\nu}(k_0, k) - D_A^{\mu\nu}(k_0, k)]$. The resummed retarded/advanced propagator is obtained by resumming the retarded/advanced gluon self energy, $\Pi_{R,A}^{\mu\nu}$. The gluon polarization tensor satisfies relations similar to those valid for the gluon propagator. In particular, the “11” component of the self energy can be written as

$$\Pi_{11}^{\mu\nu}(k_0, k) = \frac{1}{2} [\Pi_R^{\mu\nu}(k_0, k) + \Pi_A^{\mu\nu}(k_0, k) + \Pi_S^{\mu\nu}(k_0, k)] . \quad (2.3)$$

From $(\Pi_R^{\mu\nu})^* = \Pi_A^{\mu\nu}$, it follows that the discontinuity $\Pi_{11}^{\mu\nu} - (\Pi_{11}^{\mu\nu})^*$ is equal to $\Pi_S^{\mu\nu}$, since we also have that $\Pi_S^{\mu\nu}(k_0, k) = [1 + 2n_B(|k_0|)] \operatorname{sgn}(k_0) [\Pi_R^{\mu\nu}(k_0, k) - \Pi_A^{\mu\nu}(k_0, k)]$. In summary, the imaginary part of $iD_{11}^{\mu\nu}$ for spacelike momenta is proportional to $iD_S^{\mu\nu}$, which, in turn, is proportional to $\Pi_S^{\mu\nu}$. In relation to the dissociation by inelastic parton scattering indeed only $\Pi_S^{\mu\nu}$ matters, because contributions coming from the poles of the propagator are not space-like.

For the purpose of scrutinizing eq. (2.1), we will concentrate now on the case of a temporal gluon propagator in Coulomb gauge with incoming momentum $k \gg k_0$. This is the only case needed in all sections of the paper with the exception of section 7. The resummed temporal gluon propagator in Coulomb gauge is given by

$$D_{R,A}^{00}(k_0, k) = \frac{i}{k^2 + \Pi_{R,A}^{00}(k_0, k)} . \quad (2.4)$$

It follows that the temporal symmetric gluon propagator can be written as

$$D_S^{00}(k_0, k) = -i \frac{\Pi_S^{00}(k_0, k)}{(k^2 + \Pi_R^{00}(k_0, k))(k^2 + \Pi_A^{00}(k_0, k))} , \quad (2.5)$$

which makes clear that the imaginary part of iD_{11}^{00} for space-like momenta comes from Π_S^{00} . At one loop, $\Pi_S^{00}(k_0, k)$ is the sum of a light-quark, $\Pi_{S,q}^{00}(k_0, k)$, and a gluon contribution, $\Pi_{S,g}^{00}(k_0, k)$. We will consider them for momenta $k \gg k_0$. The symmetric gluon self energy can be computed by means of the cutting rules at finite temperature introduced in [45, 46] (see also [47, 48]). According to them, the quark contribution to the longitudinal polarization tensor reads

$$\Pi_{S,q}^{00}(k \gg k_0) = \frac{2ig^2 n_f}{\pi k} \int_{k/2}^{\infty} dq q^2 \left(1 - \frac{k^2}{4q^2}\right) n_F(q)[1 - n_F(q)] , \quad (2.6)$$

where, here and in the following, we neglect contributions of order k_0^2/k^2 or smaller; n_f is the number of light quarks in the self-energy loop. Noticing that $-T dn_F(q)/dq = n_F(q)[1 - n_F(q)]$, eq. (2.6) can be rewritten as

$$\Pi_{S,q}^{00}(k \gg k_0) = \frac{4ig^2 n_f T}{\pi k} \int_{k/2}^{\infty} dq q n_F(q) , \quad (2.7)$$

which agrees with the expression of $\Pi_{S,q}^{00}(k \gg k_0)$ that follows from eq. (45) of [12]. Similarly, the one-loop gluon contribution to the longitudinal polarization tensor in Coulomb gauge reads

$$\Pi_{S,g}^{00}(k \gg k_0) = \frac{2ig^2 N_c}{\pi k} \int_{k/2}^{\infty} dq q^2 \left(1 - \frac{k^2}{2q^2} + \frac{k^4}{8q^4}\right) n_B(q)[1 + n_B(q)] , \quad (2.8)$$

where N_c is the number of colours. Again, noticing that $-Tdn_B(q)/dq = n_B(q)[1 + n_B(q)]$, eq. (2.8) can be rewritten as

$$\Pi_{S,g}^{00}(k \gg k_0) = \frac{4ig^2 N_c T}{\pi k} \left[\frac{k^2}{8} n_B(k/2) + \int_{k/2}^{\infty} dq q \left(1 - \frac{k^4}{8q^4} \right) n_B(q) \right], \quad (2.9)$$

which also agrees with the expression of $\Pi_{S,g}^{00}(k \gg k_0)$ that follows from eq. (45) of [12].

In section 7 we will also need the symmetric transverse self-energy in the hard thermal loop (HTL) approximation $k_0, k \ll T$ [49]. It reads

$$\Pi_S^T(k_0, k) = \frac{ig^2}{\pi k} \theta(k^2 - k_0^2) \left(\frac{k_0^2}{k^2} - 1 \right) \int_0^{\infty} dq q^2 (N_c n_B(q)[1 + n_B(q)] + n_f n_F(q)[1 - n_F(q)]), \quad (2.10)$$

where $\Pi^T \equiv (\delta^{ij} - \hat{k}^i \hat{k}^j) \Pi^{ij}/2$ and we have neglected higher-order corrections in k_0/T .

Equations (2.6), (2.8) and (2.10) suggest the following form for the parton-scattering dissociation width:

$$\Gamma_{\text{HQ}} = \sum_p \int_{q_{\min}} \frac{d^3 q}{(2\pi)^3} f_p(q) [1 \pm f_p(q)] \sigma_p^{\text{HQ}}(q), \quad (2.11)$$

where the plus sign applies when the parton is a boson and the minus sign when the parton is a fermion. This expression incorporates the quantum-statistical effects both of Pauli blocking on the light-quark final states and of Bose enhancement on the gluon final states. We have set $q_{\text{in}}^0 = q_{\text{out}}^0 = q$, which is a good approximation as long as $T \gg E$, since the incoming parton is on shell (hence $q_{\text{in}}^0 = q$) and its momentum is of the order of the temperature, while the transferred energy is of the order of the binding energy. Although eqs. (2.7) and (2.9) seem to allow for a dissociation width of the form (2.1), this is actually not the case if σ_p^{HQ} has to be understood as a cross section. In fact the quantity convoluted with the distribution functions, when using (2.7) and (2.9), cannot be interpreted as a parton-heavy-quarkonium cross section as it does not follow from applying the optical theorem to a quarkonium-quarkonium amplitude. Our conclusion is therefore that eq. (2.1) in its common interpretation is not justified by QCD at finite temperature. QCD at finite temperature suggests instead formula (2.11) or its generalization for the case $q_{\text{in}}^0 \neq q_{\text{out}}^0$. In the rest of the paper, we will explicitly derive eq. (2.11) at leading order for a wide range of temperatures.

The momentum q_{\min} is equal to the absolute value of the quarkonium binding energy. As long as $T \gg E$, which will be the case for all thermal regimes discussed in this paper, we can set $q_{\min} = 0$ in the convolution integral (2.11). Corrections in q_{\min}/T are suppressed.

As a final comment, we remark that eq. (2.11) only holds in a leading-order picture, where one light parton with momentum of order T scatters off the bound state. At higher order, when more partons appear in the initial or final states, or when some of them have momenta of order gT , eq. (2.11) is no longer valid.

3 General considerations on the EFT approach

Before calculating the dissociation width and cross section in an EFT framework, we summarize here some general aspects of this framework. As mentioned in the introduction,

this approach is based on the hierarchies of non-relativistic and thermal scales typical of quarkonium in a quark-gluon plasma. For definiteness, we will assume that the non-relativistic scales, the temperature and the Debye mass are larger than the typical hadronic scale Λ_{QCD} , which justifies a perturbative treatment for all of them; this also implies that $v \sim \alpha_s$. A system whose energy scales may possibly satisfy this assumption is the bottomonium ground state at LHC [30].

In the following, we will consider several possible temperature regimes at weak coupling. We will proceed integrating out from thermal QCD all scales larger than $E \sim mv^2$. The ultimate EFT that describes $Q\bar{Q}$ pairs with momentum of order mv and energy of order mv^2 interacting with gluons and light quarks of energy and momentum of order mv^2 or smaller has the form of pNRQCD. If the temperature is larger than mv^2 , the matching coefficients of pNRQCD will depend on the temperature. At the accuracy we will need it in the following, the pNRQCD Lagrangian at weak coupling reads [13, 14]

$$\begin{aligned} \mathcal{L}_{\text{pNRQCD}} = \mathcal{L}_{\text{light}} + \int d^3r \, \text{Tr} \Big\{ S^\dagger [i\partial_0 - h_s] S + O^\dagger [iD_0 - h_o] O \\ + O^\dagger \mathbf{r} \cdot g\mathbf{E} S + S^\dagger \mathbf{r} \cdot g\mathbf{E} O + \frac{1}{2} O^\dagger \{ \mathbf{r} \cdot g\mathbf{E}, O \} \Big\}, \end{aligned} \quad (3.1)$$

where $\mathcal{L}_{\text{light}}$ is the part of the Lagrangian that describes the propagation of light quarks and gluons, $S = S \mathbf{1}_c / \sqrt{N_c}$ and $O = \sqrt{2} O^a T^a$ are the $Q\bar{Q}$ colour-singlet and colour-octet fields respectively, \mathbf{E} is the chromoelectric field and $iD_0 O = i\partial_0 O - gA_0 O + O gA_0$. The trace is over colour and spin indices. Gluon fields depend only on the centre-of-mass coordinate and on time. In (3.1) we have neglected irrelevant operators of order r^2 , $1/m$ or smaller; we have also neglected quantum corrections to the matching coefficients of the dipole operators, which are of order α_s or smaller, and beyond our accuracy. In the centre-of-mass frame, the singlet and octet Hamiltonians have the form ($\mathbf{p} \equiv -i\nabla_{\mathbf{r}}$):

$$h_{s,o} = \frac{\mathbf{p}^2}{m} + V_{s,o}^{(0)} + \frac{V_{s,o}^{(1)}}{m} + \frac{V_{s,o}^{(2)}}{m^2} + \dots, \quad (3.2)$$

where the dots stand for higher-order terms in the $1/m$ expansion. The first two terms in the right-hand side, which are the kinetic energy and the static potential respectively, constitute the leading-order Hamiltonian.

We refer to [12, 44] for details on pNRQCD in the context of the real-time formalism of thermal field theory. We only mention that the “2” $Q\bar{Q}$ fields decouple, hence all singlet and octet $Q\bar{Q}$ fields appearing in pNRQCD amplitudes have to be understood as “1” fields.

4 The $T \gg mv \sim m_D$ case

In the same framework that we adopt here, the case $T \gg mv \sim m_D$ was studied in section VI of [12] and in section V B of [11]. Since $m \gg T$, we start by integrating out from QCD the mass scale, obtaining NRQCD. Then we integrate out the scale T from NRQCD to arrive at a version of NRQCD that is modified by the temperature. In particular, the gauge and light-quark degrees of freedom are described by the hard thermal

loop Lagrangian [50, 51], whereas the heavy-quark sector is not modified at leading order.² The next step consists in integrating out also the scales mv and m_D to obtain a version of pNRQCD specific for the hierarchy $T \gg mv \sim m_D$.³ This version of pNRQCD corresponds to the Lagrangian (3.1), with $\mathcal{L}_{\text{light}}$ given by the HTL Lagrangian and with thermally modified $Q\bar{Q}$ potentials. In particular, $V_s^{(0)}$ is at leading order the potential computed in [6]; it reads

$$V_s^{(0)}(r) = -C_F \alpha_s \left(\frac{e^{-m_D r}}{r} + m_D \right) + i2C_F \alpha_s T \int_0^\infty dt \left(\frac{\sin(m_D r t)}{m_D r t} - 1 \right) \frac{t}{(t^2 + 1)^2}, \quad (4.1)$$

where $C_F = (N_c^2 - 1)/(2N_c)$ and

$$m_D^2 = \frac{g^2 T^2}{3} \left(N_c + \frac{n_f}{2} \right). \quad (4.2)$$

The imaginary part of eq. (4.1) describes precisely the physics of dissociation by inelastic parton scattering. Corrections of higher order in $1/m$ and g are beyond the accuracy of this paper.

At leading order in the multipole expansion, the equation of motion for the singlet field resulting from the pNRQCD Lagrangian is a Schrödinger equation with the potential, provided by eq. (4.1), consisting of a real and an imaginary part. As discussed in [12], if $mv \sim m_D$ the latter is larger than the former by a factor of T/m_D and the bound state can be considered dissociated. On the other hand, if mv is sufficiently larger than m_D , corresponding to the situation $T \gg mv \gg m_D$, then both the imaginary part and the screening are perturbations of the Coulomb potential [11, 12]. The temperature at which the real and imaginary parts become of the same size can be defined as the *dissociation temperature* T_d . One then has $T_d \sim mg^{4/3}$ [11, 15] (see also [53] for numerical estimates of the $\Upsilon(1S)$ dissociation temperature).

We derive now the cross section and decay width from the potential (4.1) under the assumption that the real part of the potential is larger than its imaginary part. At leading order, the decay width is given by

$$\Gamma_{nl} = -\langle n, l | 2 \text{Im} V_s^{(0)}(r) | n, l \rangle, \quad (4.3)$$

where $|n, l\rangle$ is an eigenstate of $\mathbf{p}^2/m + \text{Re} V_s^{(0)}(r)$, and n, l are the principal and orbital angular momentum quantum numbers identifying the quarkonium. From eq. (4.1), it follows that

$$-2 \text{Im} V_s^{(0)}(r) = \frac{g^2 T C_F m_D^2}{\pi} \int_0^\infty \frac{dt t}{(t^2 + m_D^2)^2} \left(1 - \frac{\sin(tr)}{tr} \right). \quad (4.4)$$

² This thermal version of NRQCD was called NRQCD_{HTL} in [44, 52]. In the abelian case the corresponding EFT was named NRQED_T in [53].

³ This version of pNRQCD was called pNRQCD_{HTL} in [52]. In the abelian case the corresponding EFT was named pNRQED_T in [53]. In [44] it was instead named pNRQCD_{m_D}. We also remark that in the literature there exist two versions of pNRQCD_{HTL}, one for $T \gg mv$, corresponding to the present case, and one for $mv \gg T$, which was studied in detail in [27, 54].

We observe that, given eq. (4.2), the imaginary part of the potential can be separated in a part coming from the scattering with light quarks and in a part coming from the scattering with gluons. More in detail, following the arguments of section 2, the imaginary part originates from the symmetric part of the longitudinal propagator taken in the HTL limit, $k_0, k \ll T$. The longitudinal propagator is given by eq. (2.5). The longitudinal polarization tensor, $\Pi_S^{00}(k_0, k)$, in the HTL limit follows from eqs. (2.6) and (2.8) expanded for $k_0, k \ll T$. For the quark contribution we have

$$-\frac{ik}{2\pi T}\Pi_{S,q}^{00}(k_0=0, k \ll T) = \frac{2g^2 n_f}{T} \int \frac{d^3 q}{(2\pi)^3} n_F(q) [1 - n_F(q)] = m_D^2|_{\text{quark}}, \quad (4.5)$$

where $m_D^2|_{\text{quark}} = g^2 n_f T^2/6$. For the gluon contribution we have

$$-\frac{ik}{2\pi T}\Pi_{S,g}^{00}(k_0=0, k \ll T) = \frac{2g^2 N_c}{T} \int \frac{d^3 q}{(2\pi)^3} n_B(q) [1 + n_B(q)] = m_D^2|_{\text{gluon}}, \quad (4.6)$$

where $m_D^2|_{\text{gluon}} = g^2 N_c T^2/3$. We can then rewrite the width as

$$\Gamma_{nl} = \int \frac{d^3 q}{(2\pi)^3} \left[n_F(q)(1 - n_F(q)) \langle n, l | \Sigma_q(r, q) | n, l \rangle + n_B(q)(1 + n_B(q)) \langle n, l | \Sigma_g(r, q) | n, l \rangle \right], \quad (4.7)$$

where

$$\Sigma_q(q, r) = 32\pi C_F n_f \alpha_s^2 \int_0^\infty \frac{dt t}{(t^2 + m_D^2)^2} \left(1 - \frac{\sin(tr)}{tr} \right), \quad (4.8)$$

and

$$\Sigma_g(q, r) = 32\pi C_F N_c \alpha_s^2 \int_0^\infty \frac{dt t}{(t^2 + m_D^2)^2} \left(1 - \frac{\sin(tr)}{tr} \right). \quad (4.9)$$

Finally, we can identify

$$\sigma_p^{nl}(q) = \langle n, l | \Sigma_p(r, q) | n, l \rangle, \quad (4.10)$$

with the cross section of a quarkonium state (with quantum numbers n, l) with a parton $p = q, g$ in the medium, and arrive at the formula (2.11). Note that the gluon- and quark-induced cross sections differ only in the colour structure.

We conclude this section with some comments about the cross sections. First, we note that $\Sigma_p(q, r)$ and hence the cross sections $\sigma_p^{nl}(q)$ do not depend on the parton momentum, $q \sim T$. This holds at leading order for momenta such that $m \gg q \gg mv$. As can be seen from eqs. (2.6) and (2.8), it is a consequence of assuming the temperature to be much larger than the other scales, mv, m_D and E . We also remark that the cross sections depend on the temperature only through the Debye mass, m_D . Hence, in contrast to what happens for the gluo-dissociation cross section [29], we cannot relate the cross section for inelastic parton scattering, not even at leading order, with a zero temperature process. The underlying reason is the infrared sensitivity of the cross section at the momentum scale mv , which can be seen by putting $m_D = 0$ in eqs. (4.8) and (4.9). This infrared sensitivity is cured by the HTL resummation at the scale m_D , as it will become more apparent in the next section.

4.1 The $mv \gg m_D$ case

We consider now the cross section and decay width of a quarkonium state in the special case $mv \gg m_D$. Under this condition the state is Coulombic, i.e. $\text{Re } V_s^{(0)}(r) \approx -C_F \alpha_s / r$. This case may be possibly realized only for a quarkonium $1S$ state [30], which we are going to consider in the following. The $1S$ wave function is given by $\langle \mathbf{r} | 1S \rangle = 1/(\sqrt{\pi} a_0^{3/2}) \exp(-r/a_0)$, where $a_0 = 2/(m C_F \alpha_s)$ is the Bohr radius. The evaluation of the dissociation cross section follows then easily from

$$\langle 1S | \frac{\sin(tr)}{tr} | 1S \rangle = \frac{16}{(t^2 a_0^2 + 4)^2}. \quad (4.11)$$

In particular, the light-quark cross section becomes

$$\sigma_q^{1S}(q) = \langle 1S | \Sigma_q(r, q) | 1S \rangle = 8\pi C_F n_f \alpha_s^2 a_0^2 f(m_D a_0), \quad (4.12)$$

where

$$f(x) = \frac{2}{x^2} \left[1 - 4 \frac{x^4 - 16 + 8x^2 \ln(4/x^2)}{(x^2 - 4)^3} \right], \quad (4.13)$$

and a very similar formula holds for the gluon cross section:

$$\sigma_g^{1S}(q) = \langle 1S | \Sigma_g(r, q) | 1S \rangle = 8\pi C_F N_c \alpha_s^2 a_0^2 f(m_D a_0). \quad (4.14)$$

It is convenient to define the constants

$$\sigma_{cq} \equiv 8\pi C_F n_f \alpha_s^2 a_0^2, \quad (4.15)$$

and

$$\sigma_{cg} \equiv 8\pi C_F N_c \alpha_s^2 a_0^2, \quad (4.16)$$

so that $\sigma_p^{1S} = \sigma_{cp} f(m_D a_0)$, with $p = g, q$. Plugging eqs. (4.12) and (4.14) into eq. (4.7), we obtain the width, which reads

$$\Gamma_{1S} = 2C_F \alpha_s T \left[1 - 4 \frac{(m_D a_0)^4 - 16 + 8(m_D a_0)^2 \ln(4/(m_D a_0)^2)}{((m_D a_0)^2 - 4)^3} \right]. \quad (4.17)$$

The width in this regime was already obtained in eq. (1.7) of [55]. Our result appears to be larger by a factor of 2 due to the fact that in [55] the width is defined as one half of ours. Under the assumption $mv \gg m_D$ we can further expand $f(m_D a_0)$ for $m_D a_0 \ll 1$, obtaining for the cross section

$$\sigma_p^{1S}(q) = \sigma_{cp} \left(\ln \frac{4}{m_D^2 a_0^2} - \frac{3}{2} \right), \quad \text{with } p = q, g, \quad (4.18)$$

and for the decay width

$$\Gamma_{1S} = C_F \alpha_s T m_D^2 a_0^2 \left(\ln \frac{4}{m_D^2 a_0^2} - \frac{3}{2} \right). \quad (4.19)$$

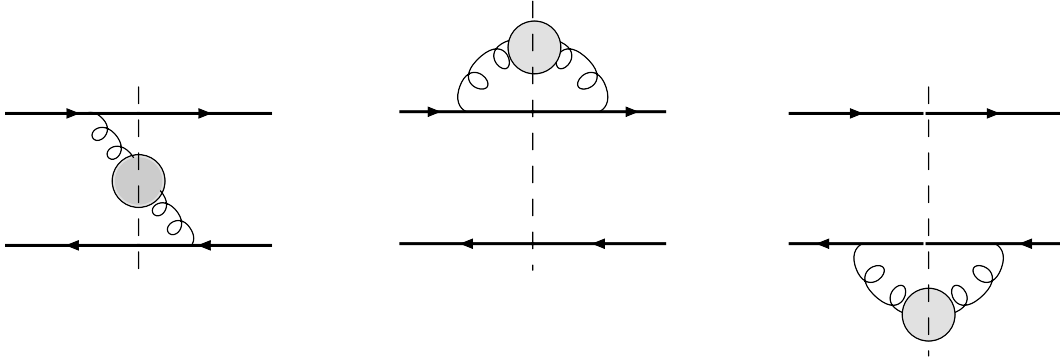


Figure 2. Cut diagrams in NRQCD. The momentum of the cut partons is of order T . Dashed lines stand for the cuts, thick lines with arrows for heavy quarks and antiquarks, curly lines for gluons and grey blobs for either light-quark or gluon loops.

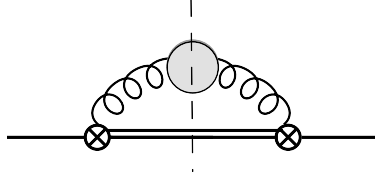


Figure 3. Cut diagram in pNRQCD. The momentum of the cut partons is of order T . The single line stands for a $Q\bar{Q}$ pair in a colour-singlet configuration, the double line for a $Q\bar{Q}$ pair in a colour-octet configuration, the circle with a cross for a chromoelectric dipole vertex, the curly line for a HTL gluon and the grey blob for either a light-quark or a gluon loop.

An alternative derivation of the cross section and decay width given in eqs. (4.18) and (4.19) consists in assuming right from the start that $T \gg mv \gg m_D$ and in evaluating the potential through the hierarchy of EFTs introduced in section VI E of [12]. It was shown there that the potential, as defined in the ultimate EFT, receives a contribution from the scale mv and one from the scale m_D . The leading-order real part of the static potential is the Coulomb potential, which comes from the scale mv . For what concerns the imaginary part of the static potential, the contribution from the scale mv is infrared divergent and originates from the cut diagrams in figure 2 when the momentum flowing in the gluon is of order mv . It reads in dimensional regularization (D is the number of spacetime dimensions)

$$\text{Im } V^{mv}(r) = \frac{C_F}{6} \alpha_s r^2 T m_D^2 \left(\frac{2}{4-D} + \gamma_E + \ln \pi + \ln(r\mu)^2 - 1 \right), \quad (4.20)$$

where γ_E is the Euler–Mascheroni constant and μ is the subtraction scale. The contribution from the scale m_D arises from the cut diagram in figure 3, where the displayed gluon stands for a HTL-resummed gluon carrying a momentum of order m_D . The gluon interacts with the $Q\bar{Q}$ field through the chromoelectric dipole interactions induced by the (second line of the) Lagrangian (3.1). The diagram was evaluated in eq. (87) of [12] and found to be

ultraviolet divergent. It gives

$$\text{Im } V^{m_D}(r) = -\frac{C_F}{6} \alpha_s r^2 T m_D^2 \left(\frac{2}{4-D} - \gamma_E + \ln \pi + \ln \frac{\mu^2}{m_D^2} + \frac{5}{3} \right), \quad (4.21)$$

which holds at leading order in an expansion in E/m_D .⁴ At this order the octet propagator in figure 3 can be taken to be $1/(-k_0 + i\epsilon)$, where k_μ is the gluon momentum; this means that the rescattering of the unbound final-state heavy quarks can be neglected. Summing the two contributions the divergence and related μ dependence cancel and one obtains

$$\text{Im } V^{mv \gg m_D}(r) \equiv \text{Im } V^{mv}(r) + \text{Im } V^{m_D}(r) = \frac{C_F}{6} \alpha_s r^2 T m_D^2 \left(2\gamma_E + \ln(r m_D)^2 - \frac{8}{3} \right). \quad (4.22)$$

Using

$$\langle 1S | r^2 | 1S \rangle = 3a_0^2, \quad (4.23)$$

and

$$\langle 1S | r^2 \ln \left(\frac{r}{a_0} \right) | 1S \rangle = 3a_0^2 \left(\frac{25}{12} - \gamma_E - \ln 2 \right), \quad (4.24)$$

from (4.3) the thermal width (4.19) and the dissociation cross section (4.18) follow.

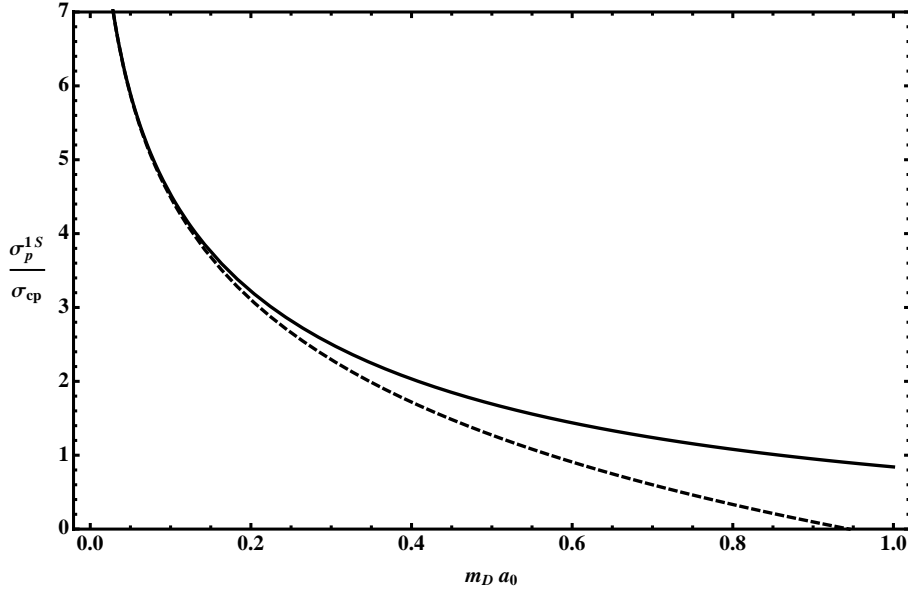


Figure 4. The rescaled cross sections $\sigma_p^{1S}/\sigma_{cp}$ as a function of $m_D a_0$. The continuous line corresponds to $f(m_D a_0)$, as defined in eq. (4.13), whereas the dashed line follows from eq. (4.18) and is thus the expansion of $f(m_D a_0)$ for $m_D a_0 \ll 1$.

In figure 4 we plot the rescaled cross section $\sigma_p^{1S}/\sigma_{cp}$, obtained in eqs. (4.12) and (4.14), as well as its expansion for $m_D a_0 \ll 1$, obtained in eq. (4.18). They are the continuous and dashed curve respectively. The two curves overlap up to $m_D a_0 \approx 0.2$. We

⁴ The condition $T \gg mv$ implies $m_D \gg E$ for a Coulombic bound state in a weakly-coupled plasma.

note that the curves have physical meaning only for values of $m_D a_0$ significantly smaller than 1. The reasons are that the dashed curve has been obtained as the leading term of an expansion in $m_D a_0$, and the continuous curve, although following from the imaginary part of the potential (4.1), which is valid also for $m_D a_0 \approx 1$, assumes the bound state to be Coulombic, see eq. (4.11), which is instead a valid assumption only for $m_D a_0$ much smaller than 1.

4.2 Comparison with the literature

As we have already mentioned, dissociation by inelastic parton scattering was first considered in the context of heavy-ion collisions in [25]. There the cross section was approximated by twice the parton heavy-quark scattering cross section computed in [34], an approximation called quasi-free approximation, complemented by the addition of momentum-independent thermal masses. The only dependence on the bound-state properties comes through q_{\min} , which was obtained from an in-medium binding energy calculated from a phenomenological potential model.

The parton heavy-quark scattering cross section corresponds to the square of the first two diagrams in figure 1. Conversely, the optical theorem relates the cross sections that we have computed in section 4 with the square of the sum of the diagrams shown in figure 5. Each of these diagrams individually corresponds to those computed in [34], however, once the square is taken, interference terms appear in the form of diagrams with gluons attached to different heavy-quark lines. These terms are the ones that are sensitive to the spatial separation between the heavy quark and antiquark, and ultimately to the bound state. The quasi-free approximation consists in neglecting these interference terms.

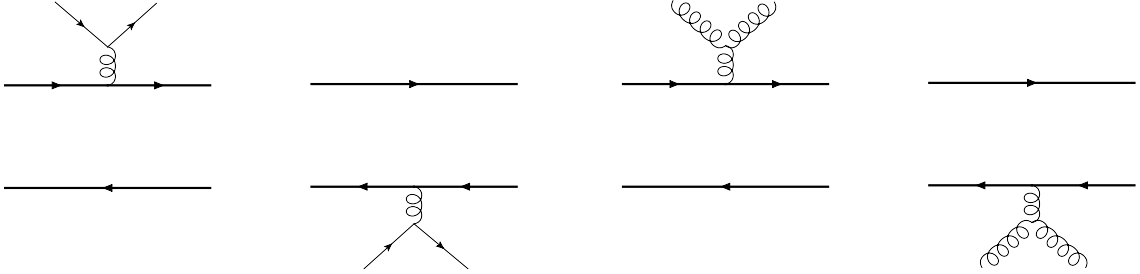


Figure 5. Diagrams contributing to the (amplitude of the) dissociation cross sections derived in section 4 and given by eq. (4.10). The thick lines represent heavy quarks and antiquarks while the thinner lines represent light quarks from the medium.

More precisely, in the right-hand side of eq. (4.4), the term proportional to $\sin(tr)/(tr)$ is the interference term while the remaining term comes from the last two cutting diagrams shown in figure 2. These two distinct terms may be traced in the cross sections. For instance, in the Coulombic case, $mv \gg m_D$, we have that, in the right-hand side of eq. (4.13), the term $2/x^2$ is the contribution from twice the square of the parton heavy-quark scattering diagram, whereas the remaining terms, which are neglected in the quasi-free approximation, are the interference terms and give a non-trivial dependence on the

wave function and thus on the properties of the bound state. In figure 6 we plot for comparison $\sigma_p^{1S}/\sigma_{cp} = f(m_D a_0)$ and the quasi-free term $2/(m_D a_0)^2$. For small values of $m_D a_0$, where (4.12) and (4.14) are valid, the quasi-free approximation overestimates the cross section by more than one order of magnitude. Conversely, for large values of $m_D a_0$, where the quasi-free approximation is sensible, the two curves overlap. In this region, however, we cannot treat the quarkonium as a Coulombic bound state, and, therefore, eqs. (4.12) and (4.14) are no longer valid.

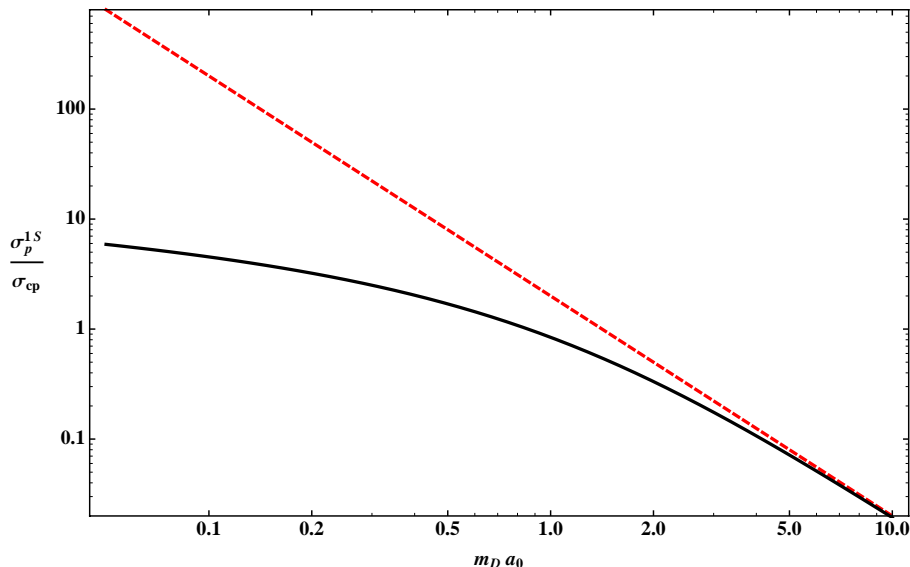


Figure 6. The rescaled cross section $\sigma_p^{1S}/\sigma_{cp}$ as a function of $m_D a_0$. The continuous line corresponds to $f(m_D a_0)$, as defined in eq. (4.13), whereas the red dashed line corresponds to $2/(m_D a_0)^2$, which is the only term that survives in the quasi-free approximation.

It is furthermore important to note that under the condition $mv \gg m_D$ the parton heavy-quark scattering contribution to the dissociation cross section is exactly cancelled at leading order in $m_D a_0$ by a contribution coming from the interference terms. The remnant of this cancellation, which is entirely due to interference/bound-state terms, is what makes up for eq. (4.18). The cancellation was noticed in [12, 56].

In summary, the quasi-free approximation is justified when all relevant thermal scales and, in particular, m_D are much larger than mv . However, in a weak-coupling regime, the condition $m_D \gg mv$ requires a temperature $T \gg mg$, which is parametrically larger than the dissociation temperature $T_d \sim mg^{4/3}$. On the other hand, whenever $m_D \ll mv$, not only the quasi-free approximation is not justified, but its contribution is exactly cancelled by bound-state effects. We conclude, therefore, that, at least in a weak-coupling framework, the quasi-free approximation is not justified for all range of temperatures where a quarkonium can exist.

5 The $T \sim mv \gg m_D$ case

The temperature region $T \sim mv \gg m_D$ was studied in detail for the case of muonic hydrogen in [53]. In the muonic hydrogen case, which may be interpreted as an abelian version of heavy quarkonium, thermal corrections are encoded in electron loops. In [53] both the real and the imaginary part of the potential were computed. Here we focus on the imaginary part of the potential, which is the quantity relevant for dissociation; thermal corrections are encoded in light-quark and gluon loops.

Let us briefly sketch our procedure. Since $m \gg T$ we can use NRQCD as a starting point. Then, as $T \sim mv$, these two scales have to be integrated out at the same time. In doing so we go from NRQCD to a new particular thermal version of pNRQCD. In the light-quark and gluon sector it is made of the HTL Lagrangian. In the heavy-quark sector the Lagrangian is as in (3.1) with the potential of a form specific to the hierarchy $T \sim mv \gg m_D$. It is at leading order a Coulomb potential that receives small corrections with a complicated functional dependence on the temperature. A feature of these thermal corrections is that they are infrared divergent. The infrared divergence that we observe in the imaginary part of the potential cancels against ultraviolet divergent contributions coming from the scale m_D , exactly as in the previous section. We discuss first light-quark and then gluon contributions.

The leading light-quark contribution to the imaginary part of the static potential comes from the one-loop fermion contribution to the diagrams in figure 2. At this order only the coupling of the heavy quarks with temporal gluons is relevant. Hence, we may follow the discussion of section 2, and the contribution reads

$$\begin{aligned} \text{Im } V_q^T(r) &= -\frac{1}{2} \text{Im } \mu^{4-D} \int \frac{d^{D-1}k}{(2\pi)^{D-1}} \left(e^{i\mathbf{k}\cdot\mathbf{r}} - 1 \right) i g^2 C_F \frac{i \Pi_{S,q}^{00}(k_0=0, k)}{k^4} \\ &= 2\pi g^4 C_F n_f \int \frac{d^3q}{(2\pi)^3} n_F(q) [1 - n_F(q)] \mu^{4-D} \int_{2q \geq k} \frac{d^{D-1}k}{(2\pi)^{D-1}} \frac{e^{i\mathbf{k}\cdot\mathbf{r}} - 1}{k^5} \left(1 - \frac{k^2}{4q^2} \right), \end{aligned} \quad (5.1)$$

where we have used the symmetric longitudinal polarization tensor given in eq. (2.6). The integral in k has an infrared divergence that we have regulated in dimensional regularization. This divergence cancels against contributions coming from the scale m_D . The contributions from the scale m_D can be evaluated from the cut diagram in figure 3 when the momentum flowing in the loop is of the order of the Debye mass. Since $E \sim m\alpha_s^2$ is parametrically smaller than m_D (exactly by one power of g), we can expand the intermediate octet propagator for $E \ll m_D$ neglecting rescattering effects and the result is the same as in eq. (4.21). Because that equation sums the contribution of quarks and gluons into m_D^2 , we need to use eqs. (4.2) and (4.5) to disentangle the one from the other. Summing the quark contribution from the scales $T \sim mv$ with the quark contribution from the scale m_D the divergences cancel and the light-quark contribution to the imaginary part of the

potential reads

$$\begin{aligned} \text{Im } V_q^{T \sim mv}(r) \equiv \text{Im } V_q^T(r) + \text{Im } V^{m_D}(r)|_{\text{quark}} = & -\frac{g^4 C_F n_f}{\pi} \left\{ \frac{r^2 T^3}{144} \left(\frac{8}{3} - 2\gamma_E - \ln(r^2 m_D^2) \right) \right. \\ & \left. + \int \frac{d^3 q}{(2\pi)^3} n_F(q) [1 - n_F(q)] \left[\int_{2q}^{\infty} \frac{dt}{t^3} \left(\frac{\sin(tr)}{tr} - 1 \right) + \int_0^{2q} \frac{dt}{4tq^2} \left(\frac{\sin(tr)}{tr} - 1 \right) \right] \right\}. \end{aligned} \quad (5.2)$$

The decay width follows from eq. (4.3). It can be written in the form of eq. (4.7), with

$$\begin{aligned} \Sigma_q(r, q) = \frac{g^4 C_F n_f r^2}{3\pi} \left[\frac{4}{3} - \gamma_E - \ln(r m_D) + \frac{6}{r^2} \int_{2q}^{\infty} \frac{dt}{t^3} \left(\frac{\sin(tr)}{tr} - 1 \right) \right. \\ \left. + \frac{3}{2q^2 r^2} \int_0^{2q} \frac{dt}{t} \left(\frac{\sin(tr)}{tr} - 1 \right) \right]. \end{aligned} \quad (5.3)$$

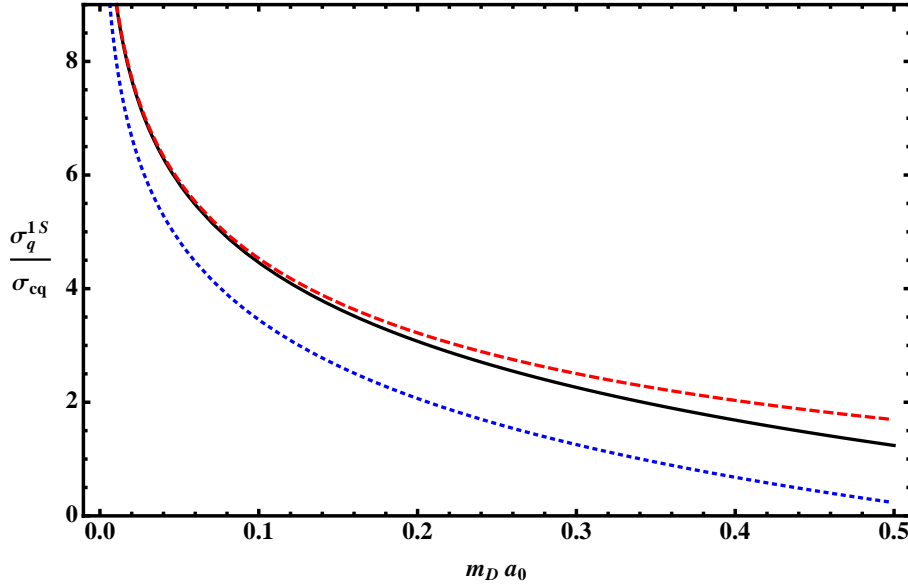


Figure 7. Comparison between the rescaled cross sections $\sigma_q^{1S}/\sigma_{cq}$ for $T \gg mv \sim m_D$ and $T \sim mv \gg m_D$, corresponding to eqs. (4.12) and (5.4) respectively. The dashed red line is the function $f(m_D a_0)$, the black continuous line is the function $h_q(m_D a_0, 10)$ and the dotted blue line is $h_q(m_D a_0, 1)$.

For $T \sim mv \gg m_D$, the cross section of a weakly-coupled $1S$ quarkonium state with light quarks from the medium is given by

$$\sigma_q^{1S}(q) = \sigma_{cq} h_q(m_D a_0, q a_0), \quad (5.4)$$

where

$$h_q(x, y) = -\ln\left(\frac{x^2}{4}\right) - \frac{3}{2} + \ln\left(\frac{y^2}{1+y^2}\right) - \frac{1}{2y^2} \ln(1+y^2), \quad (5.5)$$

σ_{cq} is defined as in eq. (4.15) and we have made use of the matrix elements computed in eqs. (4.11), (4.23) and (4.24). In the previous section we derived that, in the case $T \gg mv \sim m_D$, $\sigma_q^{1S}(q) = \sigma_{cq} f(m_D a_0)$, with f given in eq. (4.13). For $T \sim mv \gg m_D$, and differently from the case $T \gg mv \sim m_D$, the cross section depends on the momentum. However, since $T \sim mv \gg m_D$ implies that $m_D a_0 \ll 1$ and $q a_0 \sim 1$, in the limit $m_D a_0 \rightarrow 0$ and $q a_0 \rightarrow \infty$ the functions f and h_q should coincide. This can be seen in figure 7, where we have plotted h_q as a function of $m_D a_0$ for $q a_0 = 10$ (for larger values of $q a_0$ the plot would not change significantly). The residual difference between $f(m_D a_0)$ and $h_q(m_D a_0, 10)$ for moderate values of $m_D a_0$ is due to the fact that in computing f we have resummed the HTL interaction while in computing h_q we have not; the difference is however a small perturbation as long as $m_D a_0 \ll 1$.

The leading gluon contribution to the imaginary part of the static potential can be computed similarly to the quark contribution. From the scale T , we have

$$\begin{aligned} \text{Im } V_g^T(r) &= -\frac{1}{2} \text{Im } \mu^{4-D} \int \frac{d^{D-1}k}{(2\pi)^{D-1}} \left(e^{i\mathbf{k}\cdot\mathbf{r}} - 1 \right) i g^2 C_F \frac{i \Pi_{S,g}^{00}(k_0=0, k)}{k^4} \\ &= 2\pi g^4 C_F N_c \int \frac{d^3q}{(2\pi)^3} n_B(q) [1 + n_B(q)] \mu^{4-D} \int_{2q \geq k} \frac{d^{D-1}k}{(2\pi)^{D-1}} \frac{e^{i\mathbf{k}\cdot\mathbf{r}} - 1}{k^5} \left(1 - \frac{k^2}{2q^2} + \frac{k^4}{8q^4} \right), \end{aligned} \quad (5.6)$$

where we have used the symmetric longitudinal polarization tensor given in eq. (2.8). As in the quark case, the integral in k has an infrared divergence that cancels against the contribution coming from the scale m_D . The contribution from the scale m_D is given in eq. (4.21), whose gluonic part can be disentangled by means of eqs. (4.2) and (4.6). Summing the gluon contribution from the scales $T \sim mv$ with the gluon contribution from the scale m_D the complete leading-order gluon contribution to the imaginary part of the potential reads

$$\begin{aligned} \text{Im } V_g^{T \sim mv}(r) &\equiv \text{Im } V_g^T(r) + \text{Im } V^{m_D}(r)|_{\text{gluon}} = -\frac{g^4 C_F N_c}{\pi} \left\{ \frac{r^2 T^3}{72} \left(\frac{8}{3} - 2\gamma_E - \ln(r^2 m_D^2) \right) \right. \\ &+ \int \frac{d^3q}{(2\pi)^3} n_B(q) [1 + n_B(q)] \left[\int_{2q}^{\infty} \frac{dt}{t^3} \left(\frac{\sin(tr)}{tr} - 1 \right) + \int_0^{2q} \frac{dt}{2tq^2} \left(\frac{\sin(tr)}{tr} - 1 \right) \right. \\ &\left. \left. - \frac{1}{4q^2} \left(\frac{\sin^2(qr)}{(qr)^2} - 1 \right) \right] \right\}. \end{aligned} \quad (5.7)$$

The decay width follows from eq. (4.3). It can be written in the form of eq. (4.7), with

$$\begin{aligned} \Sigma_g(r, q) &= \frac{g^4 C_F N_c r^2}{3\pi} \left[\frac{4}{3} - \gamma_E - \ln(r m_D) + \frac{6}{r^2} \int_{2q}^{\infty} \frac{dt}{t^3} \left(\frac{\sin(tr)}{tr} - 1 \right) \right. \\ &\left. + \frac{3}{q^2 r^2} \int_0^{2q} \frac{dt}{t} \left(\frac{\sin(tr)}{tr} - 1 \right) - \frac{3}{2q^2 r^2} \left(\frac{\sin^2(qr)}{(qr)^2} - 1 \right) \right]. \end{aligned} \quad (5.8)$$

For $T \sim mv \gg m_D$, the cross section of a weakly-coupled $1S$ quarkonium state with gluons from the medium is given by

$$\sigma_g^{1S}(q) = \sigma_{cg} h_g(m_D a_0, q a_0), \quad (5.9)$$

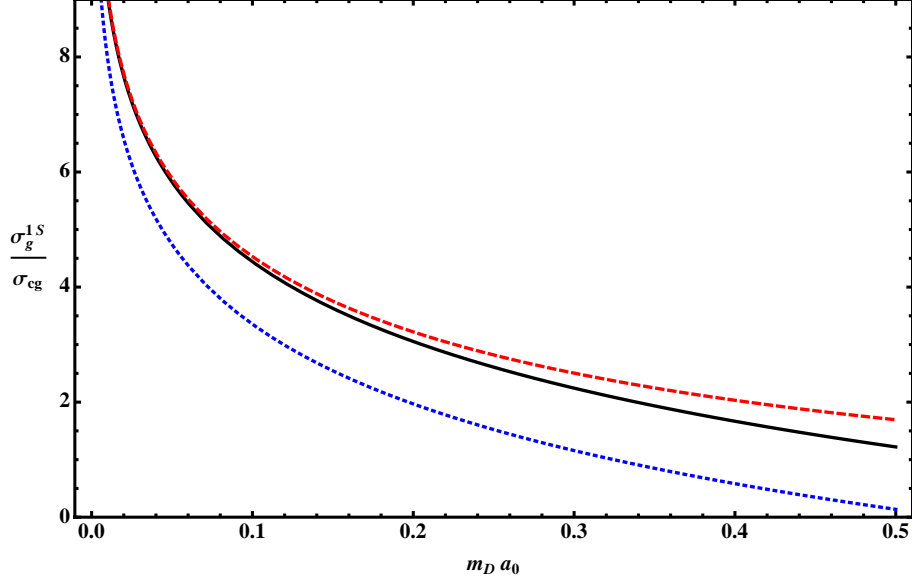


Figure 8. Comparison between the rescaled cross sections $\sigma_g^{1S}/\sigma_{cg}$ for $T \gg mv \sim m_D$ and $T \sim mv \gg m_D$, corresponding to eqs. (4.14) and (5.9) respectively. The dashed red line is the function $f(m_D a_0)$, the black continuous line is the function $h_g(m_D a_0, 10)$ and the dotted blue line is $h_g(m_D a_0, 1)$.

where

$$h_g(x, y) = -\ln\left(\frac{x^2}{4}\right) - \frac{3}{2} + \frac{1}{2(1+y^2)} + \ln\left(\frac{y^2}{1+y^2}\right) - \frac{1}{y^2} \ln(1+y^2), \quad (5.10)$$

and σ_{cg} is defined as in eq. (4.16). To obtain eq. (5.9), besides eqs. (4.11), (4.23) and (4.24), we have made use of the matrix element

$$\langle 1S | \frac{\sin^2(qr)}{(qr)^2} | 1S \rangle = \frac{1}{q^2 a_0^2 + 1}. \quad (5.11)$$

In figure 8 we plot h_g and f as a function of $m_D a_0$, and show that for large values of $q a_0$ and low values of $m_D a_0$ the cross sections calculated in this section and in section 4 overlap.

The imaginary parts of the static potential given in eqs. (5.2) and (5.7) have been calculated here for the first time. We observe that the imaginary part of the potential at the scale T , given by eqs. (5.1) and (5.6), incorporates both the effects of the free-quark-parton scattering in the \mathbf{r} -independent part and of the bound state in the \mathbf{r} -dependent part. In contrast, the contribution to the imaginary part of the potential coming from the scale m_D , given by eq. (4.21), is just an \mathbf{r} -dependent contribution, hence it would be set to zero in the quasi-free approximation.

6 The $mv \gg T \gg m_D \gg E$ case

The temperature region $mv \gg T \gg m_D \gg E$ was studied in the static case in [12]. Since thermal contributions associated with higher-order terms in the $1/m$ expansion turn out

to be suppressed, at leading order we may indeed restrict ourselves to the static case. Our procedure goes as follows. Because $mv \gg T$ we can use the pNRQCD Lagrangian at $T = 0$ as our starting point. Next we integrate out the scale T to define a version of pNRQCD specific to the hierarchy $mv \gg T$ (see footnote 3). Its Lagrangian was derived in [27, 54] and it features thermal corrections to the potentials in the heavy-quark sector and the HTL Lagrangian as $\mathcal{L}_{\text{light}}$. The correction to the colour-singlet $Q\bar{Q}$ static potential has an infrared divergence that is compensated, as in the cases previously discussed, by an ultraviolet divergence coming from the scale m_D . After integrating out m_D , we obtain a new version of pNRQCD whose potential incorporates corrections coming from the Debye-mass scale. The new potential is finite and renormalization-scheme independent. All the effects discussed in this section are specific of having an interacting $Q\bar{Q}$ system and would be absent in the quasi-free approximation.

The effect of the light-quark loop at the scale T comes from the diagram in figure 3 when the momentum flowing in the loop is of order T . Only the longitudinal part of the gluon propagator contributes and yields [12]

$$\begin{aligned} \text{Im } V_q^T(r) &= -\frac{1}{2} \mu^{4-D} \int \frac{d^D k}{(2\pi)^D} \text{Im} \left[\frac{1}{-k_0 + i\epsilon} k^2 \frac{r^2}{D-1} g^2 C_F \frac{i\Pi_{S,q}^{00}(k_0, k)}{k^4} \right] \\ &= -\frac{\pi g^4 C_F n_f r^2}{D-1} \int \frac{d^3 q}{(2\pi)^3} n_F(q) [1 - n_F(q)] \mu^{4-D} \int_{2q \geq k} \frac{d^{D-1} k}{(2\pi)^{D-1}} \frac{1}{k^3} \left(1 - \frac{k^2}{4q^2} \right), \end{aligned} \quad (6.1)$$

where we have used that $\Pi_R^{00}(k_0, k) + \Pi_A^{00}(k_0, k)$ is real and even in k_0 . The octet propagator appears in (6.1) as $1/(-k_0 + i\epsilon)$, which is again a consequence of working at leading order in $E/T \ll 1$ and neglecting rescattering effects. It is because the even part of $1/(-k_0 + i\epsilon)$ is proportional to $\delta(k_0)$ that only longitudinal gluons contribute, for the chromoelectric dipole interaction due to transverse gluons is proportional to k_0 . Equation (6.1) would also follow from expanding eq. (5.1) in r . As in that case we have regulated the infrared divergence in dimensional regularization. The contribution from the scale m_D is the one computed in eq. (4.21), whose quark and gluon contributions may be disentangled by means of eqs. (4.2), (4.5) and (4.6). The reason is again that $E/m_D \ll 1$ and we are working at leading order in E/m_D . The fact that we are working at leading order in E/T and E/m_D is ultimately also the reason why $1/m$ effects provide only subleading thermal corrections to the static result. Summing the contributions coming from the scale T and the scale m_D we get a finite expression for the light-quark contribution to the imaginary part of the potential, which, cast in (4.3), provides a thermal decay width of the form (4.7) with

$$\Sigma_q(r, q) = \frac{g^4 C_F n_f r^2}{3\pi} \left[\ln \left(\frac{2q}{m_D} \right) - 1 \right]. \quad (6.2)$$

From this it follows that the cross section of a weakly-coupled $1S$ quarkonium state with light quarks from the medium reads

$$\sigma_q^{1S}(q) = \sigma_{cq} \left[\ln \left(\frac{4q^2}{m_D^2} \right) - 2 \right], \quad (6.3)$$

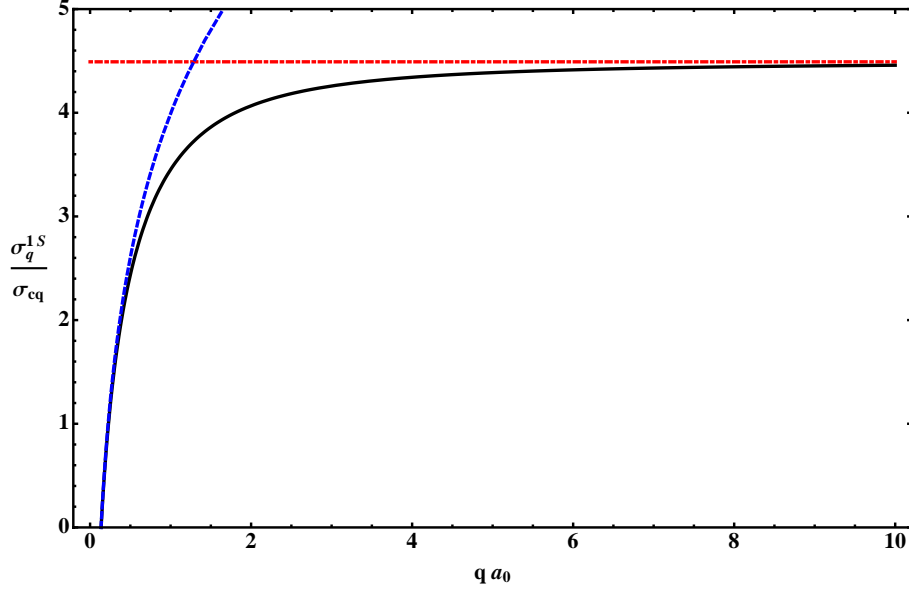


Figure 9. Rescaled dissociation cross sections due to light quarks, $\sigma_q^{1S}/\sigma_{cq}$, as a function of the rescaled momentum qa_0 . The dashed blue curve displays the cross section for $mv \gg T \gg m_D \gg E$ given in eq. (6.3), the continuous black curve displays the cross section for $T \sim mv \gg m_D$ given in eq. (5.4), and the dot-dashed red curve displays the cross section for $T \gg mv \gg m_D$ given in eq. (4.18). For all the curves we have assumed $m_D a_0 = 0.1$.

where σ_{cq} has been defined in eq. (4.15).

Performing a similar calculation for the part involving the gluon loop, at the scale T we obtain

$$\begin{aligned} \text{Im } V_g^T(r) &= -\frac{1}{2} \mu^{4-D} \int \frac{d^D k}{(2\pi)^D} \text{Im} \left[\frac{1}{-k_0 + i\epsilon} k^2 \frac{r^2}{D-1} g^2 C_F \frac{i\Pi_{S,g}^{00}(k_0, k)}{k^4} \right] \\ &= -\frac{\pi g^4 C_F N_c r^2}{D-1} \int \frac{d^3 q}{(2\pi)^3} n_B(q) (1 + n_B(q)) \mu^{4-D} \int_{2q \geq k} \frac{d^{D-1} k}{(2\pi)^{D-1}} \frac{1}{k^3} \left(1 - \frac{k^2}{2q^2} + \frac{k^4}{8q^4} \right). \end{aligned} \quad (6.4)$$

The contribution from the scale m_D is the gluonic part of eq. (4.21); summing it to eq. (6.4) we get the gluonic contribution to the imaginary part of the potential, which, cast in (4.3), provides a thermal decay width of the form (4.7) with

$$\Sigma_g(r, q) = \frac{g^4 C_F N_c r^2}{3\pi} \left[\ln \left(\frac{2q}{m_D} \right) - 1 \right]. \quad (6.5)$$

From this it follows that the cross section of a weakly-coupled $1S$ quarkonium state with gluons from the medium reads

$$\sigma_g^{1S}(q) = \sigma_{cg} \left[\ln \left(\frac{4q^2}{m_D^2} \right) - 2 \right], \quad (6.6)$$

where σ_{cg} has been defined in eq. (4.16).

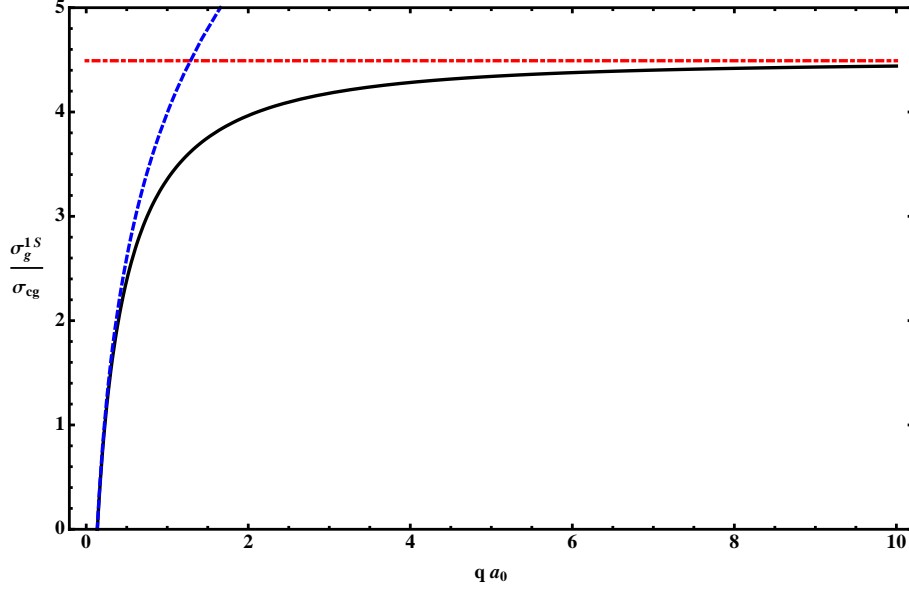


Figure 10. Rescaled dissociation cross sections due to gluons, $\sigma_g^{1S}/\sigma_{cg}$, as a function of the rescaled momentum qa_0 . The dashed blue curve displays the cross section for $mv \gg T \gg m_D \gg E$ given in eq. (6.6), the continuous black curve displays the cross section for $T \sim mv \gg m_D$ given in eq. (5.9), and the dot-dashed red curve displays the cross section for $T \gg mv \gg m_D$ given in eq. (4.18). For all the curves we have assumed $m_D a_0 = 0.1$.

We can now compare the results obtained in section 5 for $T \sim mv \gg m_D$ to the two limiting cases: $T \gg mv \gg m_D$, discussed in section 4.1, and $mv \gg T \gg m_D \gg E$, discussed here. Physically this means going from temperatures close to the dissociation temperature, T_d , to temperatures in which all the interactions with the medium can be described at leading order by a chromoelectric dipole vertex. In figure 9, we plot the three cross sections with light quarks for $m_D a_0 = 0.1$. The continuous black curve is the result for $T \sim mv \gg m_D$ as given by eq. (5.4): for $qa_0 \ll 1$ it is indeed approximated very well by the dashed blue line, which is the result for $mv \gg T \gg m_D \gg E$ just obtained in eq. (6.3); for $qa_0 \gtrsim 4$ the black line is well approximated by the constant, dot-dashed red line, which is the result for $T \gg mv \gg m_D$, as given in eq. (4.18). In figure 10, similar curves show the three cross sections with gluons.

6.1 Comparison with the literature

The results of this section bear a direct relation to the *momentum diffusion coefficient* κ of a single heavy quark, first introduced and computed in [57]. According to the field-theoretical definition of [58], the diffusion coefficient can be written as the time integral of the thermal expectation value of two chromoelectric fields linked by Wilson lines stretching along the temporal axis. Our eqs. (6.1) and (6.4) correspond indeed to the integral of the correlator of two chromoelectric fields up to a factor r^2 . Equation (B 13) of [57] matches the structure of eqs. (6.1) and (6.4), while eq. (B 14) of [57] contains the same q -dependent factor, $[\ln(4q^2/m_D^2) - 2]$, that we find in eqs. (6.3) and (6.6). Only in this section, when

the thermal scales are set between the bound state scales mv and mv^2 , which clearly do not appear in the single quark case, is this direct comparison possible. It would then be also possible to use the NLO computation of κ in [59, 60] to obtain some of the order g corrections to the width, while bound-state dependent contributions of possibly the same order, like those coming from the expansion of the octet potential, would need a new dedicated computation.⁵

7 The $mv \gg T \gg E \gg m_D$ case

The temperature region $mv \gg T \gg E \gg m_D$ was studied in detail in [27]. This temperature region is technically more difficult to treat than the other ones discussed in the paper. One of the reasons is that we find diagrams whose imaginary parts contribute both to gluo-dissociation and dissociation by inelastic parton scattering. Another reason is that the calculation of these diagrams involves not only longitudinal gluons but also transverse gluons. Since the temperature is smaller than the typical inverse radius of the quarkonium, all quarkonium interactions with the medium are described at leading order by chromoelectric dipole vertices. Hence, also the effects discussed in this section are specific of having an interacting $Q\bar{Q}$ system and would be absent in the quasi-free approximation.

Our starting point is the pNRQCD Lagrangian defined in the previous section after integrating out the temperature T . The reason we can start from there is that the Lagrangian of an EFT is only sensitive to the hierarchy of energy scales above its ultraviolet cutoff. Therefore integrating out the scales mv and T is unaffected by the relation between m_D and E . Because the Lagrangian at the scale T is the same, the leading contributions to the imaginary part of the static potential from the scale T can be read off directly from eqs. (6.1) and (6.4).

The next step consists in integrating over momenta of the order of the binding energy E . At this scale, the octet propagator in the diagram of figure 3 can no longer be taken as $1/(-k_0 + i\epsilon)$, for the momentum k_μ flowing in the loop is of the same order as the octet energy. This means that the rescattering between the unbound heavy-quarks and their relative motion has to be taken into account. As a consequence, the interaction between heavy quarks and transverse gluons, which is proportional to k_0 , does not vanish and contributes to the computation. This should be contrasted with what occurs for other energy scales.

The retarded/advanced propagator of a transverse gluon in Coulomb gauge after HTL resummation reads

$$D_{R,A}^{ij}(k_0, k) = i \frac{\delta^{ij} - \hat{k}^i \hat{k}^j}{(k_0 \pm i\epsilon)^2 - k^2 - \Pi_{R,A}^T(k_0/k)} , \quad (7.1)$$

⁵ We remark that the NLO calculation of [59, 60], when applied to heavy quarkonium, shows how the distinction between dissociation by inelastic parton scattering and gluo-dissociation fails beyond leading order. For instance, the intricate structure of cuts discussed in [59, 60] includes processes with two light partons in the initial and final state.

where $\Pi_{R,A}^T(k_0/k) = (\delta^{ij} - \hat{k}^i \hat{k}^j) \Pi^{ij}(k_0 \pm i\epsilon, k)/2$ is the HTL retarded/advanced transverse gluon self energy.⁶ It has the following properties. First, $\Pi_{R,A}^T(0) = 0$. Second, $\text{Im} \Pi_{R,A}^T(k_0/k)$ is different from 0 only for $|k_0/k| < 1$. The fact that the imaginary part of $\Pi_{R,A}^T$ does not vanish only for space-like momenta implies that it contributes only to quarkonium dissociation through inelastic parton scattering. Finally, we have that $\text{Re} \Pi_{R,A}^T(k_0/k \gtrsim 1) \sim m_D^2$. The equation $k_0^2 - k^2 - \text{Re} \Pi_{R,A}^T(k_0/k) = 0$ has then a solution only for time-like momenta. This solution is called plasmon pole and obeys a special dispersion relation with a momentum-dependent mass. For time-like momenta the imaginary part of $iD_{R,A}^{ij}$ comes only from the $i\epsilon$ prescription on the plasmon pole. Hence the plasmon pole contributes only to the quarkonium gluo-dissociation. There are two distinct momentum regions where the gluon propagator is nearly singular or singular. One is the region where $k_0 \sim k \sim E$ and $k_0^2 - k^2 \sim E^2$. In this region, which has been called off-shell region in [27], we can expand the gluon propagator in the transverse gluon self energy. The other is the region where $k_0 \sim k \sim E$ and $k_0^2 - k^2 \sim m_D^2$. In this region, which has been called collinear region in [27], HTL effects have to be resummed.

The situation at the scale E is therefore the following. Gluons interact with the $Q\bar{Q}$ pair at leading order through chromoelectric dipole interactions. The relevant Feynman diagram is shown in figure 3. Because at this scale the rescattering of the $Q\bar{Q}$ pair cannot be neglected, both longitudinal and transverse gluons contribute to the quarkonium thermal decay. Quarkonium may decay either by emitting time-like or light-like gluons, which corresponds to cutting the diagram in figure 3 along the gluon propagator and picking up its pole contribution, or by scattering with partons in the medium. This last situation corresponds to cutting the diagram in figure 3 along the gluon self-energy diagram and picking up its discontinuity, which is encoded in the symmetric polarization tensor. The momentum of the gluon is in this case space-like. According to our definitions the first decay process contributes to quarkonium gluo-dissociation whereas the second one to dissociation by inelastic parton scattering. Both decay processes are intertwined at the scale E and may be disentangled only by looking at the time-like or space-like nature of the gluon interacting with the $Q\bar{Q}$ pair. If the gluon interacting with the $Q\bar{Q}$ pair is longitudinal, then the residue of its plasmon pole contribution is exponentially suppressed for momenta $k_0 \sim k \sim E \gg m_D$ [63, 64], whereas a contribution to the thermal width comes from the imaginary part of the longitudinal polarization tensor. This is different from zero only for space-like momenta and hence contributes only to quarkonium dissociation by inelastic parton scattering. If the gluon interacting with the $Q\bar{Q}$ pair is transverse, then it may contribute either through its plasmon pole or through the imaginary part of the transverse gluon self energy. The former case, which may happen only in the collinear momentum region for time-like gluon momenta, contributes to quarkonium gluo-dissociation. The latter case, which may happen both in the collinear and in the off-shell momentum regions for space-like

⁶ The explicit expression of $\Pi_{R,A}^T$ is [61, 62]

$$\Pi_{R,A}^T(k_0/k) = \frac{m_D^2}{2} \left[\frac{k_0^2}{k^2} - \left(\frac{k_0^2}{k^2} - 1 \right) \frac{k_0}{2k} \ln \left(\frac{k_0 + k \pm i\epsilon}{k_0 - k \pm i\epsilon} \right) \right].$$

momenta, contributes to quarkonium dissociation by inelastic parton scattering. We will disentangle the gluo- and parton-scattering dissociation contributions to the cross section in the following two sections.

7.1 Gluo-dissociation

Quarkonium gluo-dissociation was studied in [29] at leading order in an m_D/E expansion, which corresponds to evaluating the diagram in figure 3 with a free gluon. Here we add HTL effects, which amounts at computing the gluo-dissociation width and cross section at NLO. It is when HTL effects are taken into account that also parton-scattering dissociation happens.

For the reasons discussed in the previous paragraphs, gluo-dissociation is due to the diagram shown in figure 3 when the gluon is transverse and its momentum time-like. The relevant contributions have been calculated in appendix A of [27]. Using those results the gluo-dissociation thermal width at next-to-leading order in m_D/E and E/T reads

$$\begin{aligned} \Gamma_{nl} = & \frac{4}{3}\alpha_s C_F T \langle n, l | r_i (E - h_o^{(0)})^2 r_i | n, l \rangle + \frac{2}{3}\alpha_s C_F \langle n, l | r_i (E - h_o^{(0)})^3 r_i | n, l \rangle \\ & - \frac{\alpha_s C_F T m_D^2}{3} \langle n, l | r_i \left[\ln \left(\frac{8(E - h_o^{(0)})^2}{m_D^2} \right) - 2 \right] r_i | n, l \rangle, \end{aligned} \quad (7.2)$$

where $h_o^{(0)} = \mathbf{p}^2/m + \alpha_s/(2N_c r)$ is the leading-order octet Hamiltonian. The first term in the right-hand side of (7.2) is the leading (zeroth-)order width in the m_D/E and E/T expansions: it reproduces the result of [29] for $T \gg E$. The other two terms are the next-to-leading-order corrections.

The gluo-dissociation width may be expressed as the convolution of a gluon-heavy-quarkonium dissociation cross section in the medium, $\sigma_{\text{gluo}}^{nl}$, and a gluon distribution function:

$$\Gamma_{nl} = \int_{q_{\min}} \frac{d^3 q}{(2\pi)^3} n_B(q) \sigma_{\text{gluo}}^{nl}(q). \quad (7.3)$$

Note that, in contrast to the parton-scattering dissociation case, described by eq. (2.11), there is just one parton of the medium involved in the gluo-dissociation process and therefore just one distribution function appearing in (7.3). Comparing (7.3) with (7.2) and expanding the Bose-Einstein distribution for $T \gg E$, we obtain the gluo-dissociation cross section

$$\sigma_{\text{gluo}}^{nl}(q) = Z(q/m_D) \sigma_{\text{gluo}}^{nl(0)}(q), \quad (7.4)$$

where $\sigma_{\text{gluo}}^{nl(0)}$ is the leading-order cross section that corresponds to the first line in the right-hand side of (7.2). Its explicit expression for a $1S$ Coulombic bound state can be found in [29, 33] and reads

$$\sigma_{\text{gluo}}^{1S(0)}(q) = \frac{\alpha_s C_F}{3} 2^{10} \pi^2 \rho (\rho + 2)^2 \frac{E_1^4}{m q^5} (t(q)^2 + \rho^2) \frac{e^{\frac{4\rho}{t(q)} \arctan(t(q))}}{e^{\frac{2\pi\rho}{t(q)}} - 1}, \quad (7.5)$$

where $\rho \equiv 1/(N_c^2 - 1)$, $t(q) \equiv \sqrt{q/|E_1| - 1}$ and $E_1 = -m C_F^2 \alpha_s^2/4$ is the energy of the first Bohr level. The absolute value of E_1 provides the low-momentum cut-off in the

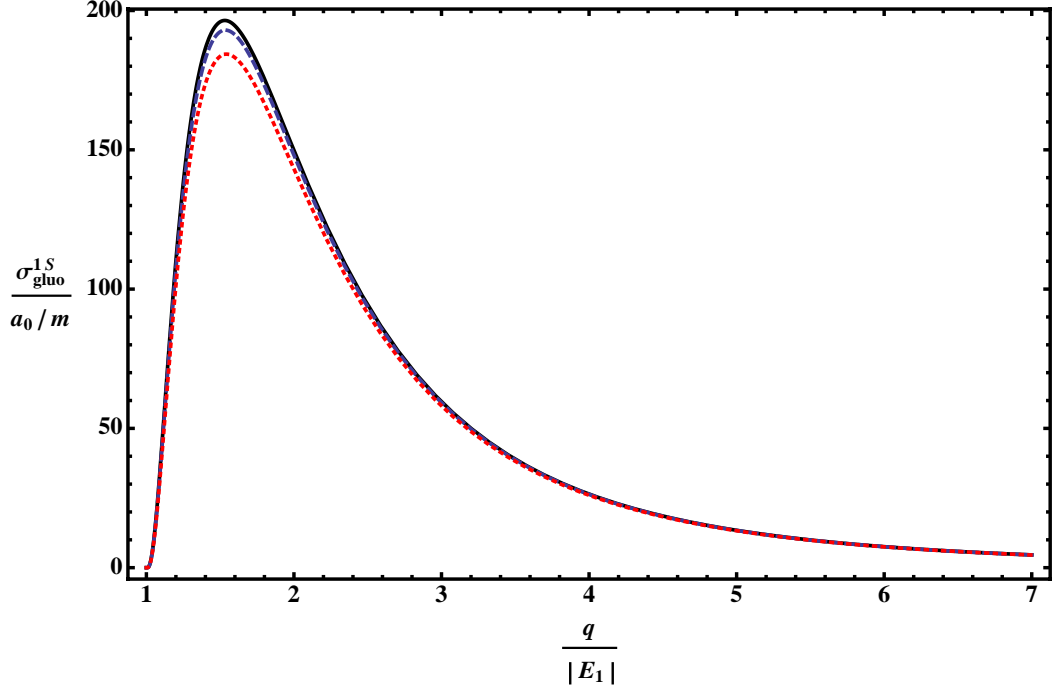


Figure 11. $1S$ gluo-dissociation cross section in units of a_0/m . The continuous black line is the leading-order result, $\sigma_{\text{gluo}}^{1S(0)}$. The dashed blue line shows $\sigma_{\text{gluo}}^{1S}$, according to eq. (7.4), for $m_D m a_0^2 = 0.2$ and the dotted red line for $m_D m a_0^2 = 0.5$.

integral (7.3). The factor Z can be understood as a wave-function normalization of the gluon due to the HTL resummation, it reads

$$Z(x) = 1 - \frac{1}{4x^2} [\ln(8x^2) - 2] . \quad (7.6)$$

The effect of the normalization factor Z on the $1S$ gluo-dissociation cross section is shown in figure 11, where the cross section is expressed in units of $a_0/m = 2/(m^2 C_F \alpha_s)$ and the gluon momentum in units of $|E_1|$. The plot shows how the HTL resummation results in a global lowering of the cross section.⁷

7.2 Dissociation by inelastic parton scattering

Contributions from the scale E to quarkonium dissociation by inelastic parton scattering come from the different sources that we have analyzed in the introduction of section 7. We have the contribution from longitudinal gluons and that from transverse gluons. The contribution from transverse gluons is divided into contributions from the collinear region and from the off-shell region, which are separated by a cut-off. Only the sum of all these contributions is gauge invariant and cut-off independent. These different contributions have all been computed: the contribution from the longitudinal gluons can be found in eq. (5.17)

⁷ $Z(q/m_D)$ becomes larger than one for $q < 2^{-3/2} e m_D \approx 0.96 m_D$. However the cross section has a threshold at $q = |E_1|$, and $|E_1|$ is larger than m_D in the assumed hierarchy.

of [27]; the contributions from the transverse gluons, of which we have to keep only the contributions coming from space-like momenta, can be found in appendix A of [27].

The final light-quark loop contribution to the decay width from the scale E is

$$\Gamma_{nl,q}^E = -\frac{g^4 C_F n_f}{3\pi} \langle n, l | r^2 | n, l \rangle \int \frac{d^3 q}{(2\pi)^3} n_F(q) (1 - n_F(q)) \left[\frac{1}{D-4} - \frac{1}{2} \ln(2\pi) + \frac{\gamma_E}{2} - \frac{5}{6} + \ln\left(\frac{m_D}{\mu}\right) \right]. \quad (7.7)$$

Adding to it the contribution from the scale T , as given by eqs. (6.1) and (4.3), the divergence cancels and we can cast the decay width in the form (4.7) with

$$\Sigma_q(r, q) = \frac{16\pi C_F n_f \alpha_s^2 r^2}{3} \left[\ln\left(\frac{2q}{m_D}\right) + \frac{\ln 2}{2} - 1 \right]. \quad (7.8)$$

For a $1S$ Coulombic state, the corresponding quark-heavy-quarkonium dissociation cross section then reads

$$\sigma_q^{1S}(q) = \sigma_{cq} \left[\ln\left(\frac{4q^2}{m_D^2}\right) + \ln 2 - 2 \right], \quad (7.9)$$

where σ_{cq} has been defined in (4.15).

The gluon loop contribution to the decay width from the scale E is the same up to a different colour structure and different distribution functions:

$$\Gamma_{nl,g}^E = -\frac{g^4 C_F N_c}{3\pi} \langle n, l | r^2 | n, l \rangle \int \frac{d^3 q}{(2\pi)^3} n_B(q) (1 + n_B(q)) \left[\frac{1}{D-4} - \frac{1}{2} \ln(2\pi) + \frac{\gamma_E}{2} - \frac{5}{6} + \ln\left(\frac{m_D}{\mu}\right) \right]. \quad (7.10)$$

Adding to it the contribution from the scale T , as given by eqs. (6.4) and (4.3), the divergence cancels and we can cast the decay width in the form (4.7) with

$$\Sigma_g(r, q) = \frac{16\pi C_F N_c \alpha_s^2 r^2}{3} \left[\ln\left(\frac{2q}{m_D}\right) + \frac{\ln 2}{2} - 1 \right]. \quad (7.11)$$

For a $1S$ Coulombic state, the corresponding gluon-heavy-quarkonium dissociation cross section then reads

$$\sigma_g^{1S}(q) = \sigma_{cg} \left[\ln\left(\frac{4q^2}{m_D^2}\right) + \ln 2 - 2 \right], \quad (7.12)$$

where σ_{cg} has been defined in (4.16).

The parton-scattering decay width is of order $\alpha_s T \times (m_D/mv)^2$, therefore suppressed by a factor $(m_D/E)^2$ with respect to the gluo-dissociation width, which at leading order scales like $\alpha_s T \times (E/mv)^2$. The parton-scattering decay width is comparable in size to the next-to-leading-order correction to the gluo-dissociation width that appears in the second line of (7.2), while the next-to-leading-order correction appearing in the first line of (7.2) is of order $\alpha_s T \times (E/mv)^2 \times (E/T)$. Hence, in the temperature region $mv \gg T \gg E \gg m_D$, dissociation by inelastic parton scattering is a subleading effect with respect to gluo-dissociation and may be neglected in first approximation. At the same time we observe

that in all other temperature regions examined in the paper we had $m_D \gg E$. Therefore, in those regions, just the opposite holds and dissociation by inelastic parton scattering is the parametrically dominant quarkonium dissociation process. These observations agree with the early findings of [12]. The dominance of dissociation by inelastic parton scattering over gluo-dissociation at high temperatures was noticed in [25, 26].

7.3 Comparison with the literature

In [37] parton-scattering and gluo-dissociation have been treated in an unified framework. We will highlight some qualitative features of that work that are common also to other approaches but that are different from the EFT treatment presented here. The first difference is that the calculation of [37] uses the formula (2.1) for both the parton-scattering and the gluo-dissociation widths. We have seen that this is consistent with QCD only in the latter case. The cross sections used in [37] have been derived from a Bethe–Salpeter framework in [35]. The calculation includes systematically bound-state effects, but with some limitations: it is valid in the large N_c limit, hence it neglects rescattering effects of the unbound colour-octet quark-antiquark pair; it describes the quarkonium interaction with gluons through chromoelectric dipole vertices, hence the description holds for gluons whose energy and momentum are smaller than mv . The cross section does not include systematically thermal effects, for it is calculated at zero temperature. Constant thermal masses have been added to regulate infrared divergences. This amounts at a phenomenological tuning: from a QCD perspective one should recall that momentum and temperature-independent masses are neither consistent with HTL resummation nor with weak-coupling perturbative calculations.

8 Conclusions

Quarkonium dissociation through scattering with light partons is one of the processes responsible for the thermal decay width of quarkonium in a deconfined medium. It is the dominant process for temperatures such that the Debye mass, m_D , is larger than the binding energy, E .

We have studied this process in a weak-coupling effective field theory framework, where quarkonium dissociation through scattering with partons in the medium may be related, for momentum transfer larger than E , to the imaginary part of the potential and the Landau damping phenomenon. We have shown that in our setting the quasi-free approximation, which consists in approximating the dissociation cross section of the quarkonium with that of two free quarks, is never a valid approximation. In particular, for momentum transfer smaller than or of the same order as the inverse radius of the quarkonium, the dissociation cross section in the quasi-free approximation is exactly cancelled by bound-state effects.

The parton-scattering dissociation cross section, valid for temperatures such that m_D is much larger than E , is of the form (4.10), with Σ_q given in (5.3) for scattering with light quarks from the medium and Σ_g given in (5.8) for scattering with gluons. In the specific case of a Coulombic $1S$ state, the cross sections with gluons and quarks are given respectively by eqs. (5.4) and (5.9) and shown by the black curves in figures 9 and 10. In the

region of temperatures where m_D is of the order of the inverse radius of the quarkonium, i.e. in the region where screening effects are important, Σ_q is given by eq. (4.8) and Σ_g by eq. (4.9). In the case of a Coulombic $1S$ state, the cross sections with quarks and gluons are given respectively by eqs. (4.12) and (4.14). The impact of the screening on the cross sections is shown in figures 7 and 8. The parton-scattering dissociation cross section has been computed also for temperatures such that m_D is much smaller than E . The light-quark contribution is given in eq. (7.8) with the corresponding cross section for a $1S$ Coulombic state in (7.9), and the gluon contribution is given in eq. (7.11) with the corresponding cross section for a $1S$ Coulombic state given in (7.12). In this temperature regime, dissociation by inelastic parton scattering is, however, a subleading effect.

From the parton-scattering dissociation cross section we may calculate the corresponding dissociation width through eq. (2.11). This expression is justified by general arguments based on the optical theorem and cutting rules at finite temperature, and by the explicit calculations performed in the paper in the different temperature regimes. Equation (2.11) should replace the widely used formula (2.1), which is justified only in the gluo-dissociation case.

Gluo-dissociation is the process occurring when a sufficiently energetic gluon of the medium is absorbed by the quarkonium and dissociates it into an unbound colour-octet $Q\bar{Q}$ pair. This is the dominant dissociation process in the temperature region where m_D is much smaller than E , while it is subleading with respect to dissociation by inelastic parton scattering if m_D is much larger than E . Gluo-dissociation has been called singlet-to-octet thermal breakup in the effective field theory literature on the subject. We have calculated the gluo-dissociation cross section in eq. (7.4) and thermal width in eq. (7.2) at next-to-leading order in m_D/E and E/T . This is currently the most accurate determination of gluo-dissociation in weak coupling, whose impact is shown in figure 11.

Acknowledgments

We acknowledge financial support from the DFG cluster of excellence *Origin and structure of the universe* (www.universe-cluster.de). This research is supported by the DFG grant BR 4058/1-1. The work of J.G. was supported by the Natural Science and Engineering Research Council of Canada and by an Institute of Particle Physics Theory Fellowship.

References

- [1] T. Matsui and H. Satz, Phys. Lett. B **178** (1986) 416.
- [2] N. Brambilla *et al.*, *Heavy quarkonium physics*, CERN-2005-005, (CERN, Geneva, 2005) [arXiv:hep-ph/0412158].
- [3] N. Brambilla *et al.*, Eur. Phys. J. C **71** (2011) 1534 [arXiv:1010.5827 [hep-ph]].
- [4] S. Chatrchyan *et al.* [CMS Collaboration], Phys. Rev. Lett. **109** (2012) 222301 [arXiv:1208.2826 [nucl-ex]]; [CMS Collaboration], CMS-PAS-HIN-12-014; CMS-PAS-HIN-12-007.

- [5] B. Abelev *et al.* [ALICE Collaboration], Phys. Rev. Lett. **109** (2012) 072301 [arXiv:1202.1383 [hep-ex]].
- [6] M. Laine, O. Philipsen, P. Romatschke and M. Tassler, JHEP **0703** (2007) 054 [arXiv:hep-ph/0611300].
- [7] Y. Burnier, M. Laine and M. Vepsalainen, JHEP **0801** (2008) 043 [arXiv:0711.1743 [hep-ph]].
- [8] P. Petreczky, C. Miao and A. Mocsy, Nucl. Phys. A **855** (2011) 125 [arXiv:1012.4433 [hep-ph]].
- [9] M. Strickland, Phys. Rev. Lett. **107** (2011) 132301 [arXiv:1106.2571 [hep-ph]].
- [10] M. Strickland and D. Bazow, Nucl. Phys. A **879** (2012) 25 [arXiv:1112.2761 [nucl-th]].
- [11] M. A. Escobedo and J. Soto, Phys. Rev. A **78** (2008) 032520 [arXiv:0804.0691 [hep-ph]].
- [12] N. Brambilla, J. Ghiglieri, A. Vairo and P. Petreczky, Phys. Rev. D **78** (2008) 014017 [arXiv:0804.0993 [hep-ph]].
- [13] A. Pineda and J. Soto, Nucl. Phys. Proc. Suppl. **64** (1998) 428 [arXiv:hep-ph/9707481].
- [14] N. Brambilla, A. Pineda, J. Soto and A. Vairo, Nucl. Phys. B **566** (2000) 275 [arXiv:hep-ph/9907240].
- [15] M. Laine, Nucl. Phys. A **820** (2009) 25C [arXiv:0810.1112 [hep-ph]].
- [16] M. Laine, O. Philipsen and M. Tassler, JHEP **0709** (2007) 066 [arXiv:0707.2458 [hep-lat]].
- [17] A. Rothkopf, T. Hatsuda and S. Sasaki, Phys. Rev. Lett. **108** (2012) 162001 [arXiv:1108.1579 [hep-lat]].
- [18] Y. Burnier and A. Rothkopf, Phys. Rev. D **86** (2012) 051503 [arXiv:1208.1899 [hep-ph]].
- [19] A. Mocsy, P. Petreczky, Phys. Rev. Lett. **99** (2007) 211602. [arXiv:0706.2183 [hep-ph]].
- [20] R. Rapp, D. Blaschke and P. Crochet, Prog. Part. Nucl. Phys. **65** (2010) 209 [arXiv:0807.2470 [hep-ph]].
- [21] L. Kluberg and H. Satz, arXiv:0901.3831 [hep-ph].
- [22] R. Rapp and H. van Hees, R. C. Hwa, X.-N. Wang (Ed.) Quark Gluon Plasma 4, World Scientific, 111 (2010) [arXiv:0903.1096 [hep-ph]].
- [23] D. Kharzeev and H. Satz, Phys. Lett. B **334** (1994) 155 [arXiv:hep-ph/9405414].
- [24] X. M. Xu, D. Kharzeev, H. Satz and X. N. Wang, Phys. Rev. C **53** (1996) 3051 [arXiv:hep-ph/9511331].
- [25] L. Grandchamp and R. Rapp, Phys. Lett. B **523** (2001) 60 [hep-ph/0103124].
- [26] L. Grandchamp and R. Rapp, Nucl. Phys. A **709** (2002) 415 [hep-ph/0205305].
- [27] N. Brambilla, M. A. Escobedo, J. Ghiglieri, J. Soto and A. Vairo, JHEP **1009** (2010) 038 [arXiv:1007.4156 [hep-ph]].
- [28] F. Riek and R. Rapp, New J. Phys. **13** (2011) 045007 [arXiv:1012.0019 [nucl-th]].
- [29] N. Brambilla, M. A. Escobedo, J. Ghiglieri and A. Vairo, JHEP **1112** (2011) 116 [arXiv:1109.5826 [hep-ph]].
- [30] A. Vairo, AIP Conf. Proc. **1317** (2011) 241 [arXiv:1009.6137 [hep-ph]].
- [31] G. Aarts, C. Allton, S. Kim, M. P. Lombardo, M. B. Oktay, S. M. Ryan, D. K. Sinclair and J. I. Skullerud, JHEP **1111** (2011) 103 [arXiv:1109.4496 [hep-lat]].

- [32] G. Bhanot and M. E. Peskin, Nucl. Phys. B **156** (1979) 391.
- [33] F. Breziniski and G. Wolschin, Phys. Lett. B **707** (2012) 534 [arXiv:1109.0211 [hep-ph]].
- [34] B. L. Combridge, Nucl. Phys. B **151** (1979) 429.
- [35] T. Song and S. H. Lee, Phys. Rev. D **72** (2005) 034002 [hep-ph/0501252].
- [36] L. Grandchamp, S. Lumpkins, D. Sun, H. van Hees and R. Rapp, Phys. Rev. C **73** (2006) 064906 [hep-ph/0507314].
- [37] Y. Park, K. I. Kim, T. Song, S. H. Lee and C. Y. Wong, Phys. Rev. C **76** (2007) 044907 [arXiv:0704.3770 [hep-ph]].
- [38] X. Zhao and R. Rapp, Phys. Rev. C **82** (2010) 064905 [arXiv:1008.5328 [hep-ph]].
- [39] A. Emerick, X. Zhao and R. Rapp, Eur. Phys. J. A **48** (2012) 72 [arXiv:1111.6537 [hep-ph]].
- [40] T. Song, K. C. Han and C. M. Ko, Phys. Rev. C **85** (2012) 014902 [arXiv:1112.0613 [nucl-th]].
- [41] W. E. Caswell and G. P. Lepage, Phys. Lett. B **167** (1986) 437.
- [42] G. T. Bodwin, E. Braaten and G. P. Lepage, Phys. Rev. D **51** (1995) 1125 [Erratum-ibid. D **55** (1997) 5853] [hep-ph/9407339].
- [43] M. Le Bellac, *Thermal field theory*, Cambridge University Press, Cambridge, 2000.
- [44] J. Ghiglieri, PhD Thesis, TU Munich, 2011, arXiv:1201.2920 [hep-ph].
- [45] R. L. Kobes and G. W. Semenoff, Nucl. Phys. B **260** (1985) 714.
- [46] R. L. Kobes and G. W. Semenoff, Nucl. Phys. B **272** (1986) 329.
- [47] P. F. Bedaque, A. K. Das and S. Naik, Mod. Phys. Lett. A **12** (1997) 2481 [hep-ph/9603325].
- [48] F. Gelis, Nucl. Phys. B **508** (1997) 483 [hep-ph/9701410].
- [49] E. Braaten and R. D. Pisarski, Nucl. Phys. B **337** (1990) 569.
- [50] E. Braaten and R. D. Pisarski, Phys. Rev. D **45** (1992) 1827.
- [51] J. Frenkel and J. C. Taylor, Nucl. Phys. B **334** (1990) 199.
- [52] A. Vairo, PoS CONFINEMENT **8** (2008) 002 [arXiv:0901.3495 [hep-ph]].
- [53] M. A. Escobedo and J. Soto, Phys. Rev. A **82** (2010) 042506 [arXiv:1008.0254 [hep-ph]].
- [54] N. Brambilla, M. A. Escobedo, J. Ghiglieri and A. Vairo, JHEP **1107** (2011) 096 [arXiv:1105.4807 [hep-ph]].
- [55] A. Dumitru, Prog. Theor. Phys. Suppl. **187** (2011) 87 [arXiv:1010.5218 [hep-ph]].
- [56] A. Beraudo, J. -P. Blaizot and C. Ratti, Nucl. Phys. A **806** (2008) 312 [arXiv:0712.4394 [nucl-th]].
- [57] G. D. Moore and D. Teaney, Phys. Rev. C **71** (2005) 064904 [hep-ph/0412346].
- [58] J. Casalderrey-Solana and D. Teaney, Phys. Rev. D **74** (2006) 085012 [hep-ph/0605199].
- [59] S. Caron-Huot and G. D. Moore, Phys. Rev. Lett. **100** (2008) 052301 [arXiv:0708.4232 [hep-ph]].
- [60] S. Caron-Huot and G. D. Moore, JHEP **0802** (2008) 081 [arXiv:0801.2173 [hep-ph]].
- [61] O. K. Kalashnikov and V. V. Klimov, Sov. J. Nucl. Phys. **31** (1980) 699 [Yad. Fiz. **31** (1980) 1357].

- [62] H. A. Weldon, Phys. Rev. D **26** (1982) 1394.
- [63] R. D. Pisarski, Physica A **158** (1989) 146.
- [64] J. -P. Blaizot and E. Iancu, Phys. Rept. **359** (2002) 355 [hep-ph/0101103].